

SCHOOL OF DENTISTRY



Research Day 2023

THURSDAY, MARCH 2

KCRB



ADA C-E-R-P® | Continuing Education Recognition Program



2023 Research Day

THURSDAY, MARCH 2

8:00 a.m. **Poster Setup**

KCRB MAIN LEVEL

8:30 a.m. **Poster Viewing and Lite Breakfast**

ENTER VIA THE
EASTSIDE/ RIVERSIDE
ENTRANCE

8:30 a.m. | Poster Session #1

9:40 a.m. | Poster Session #2

10:50 a.m. | Poster Session #3

12:00 noon **Lunch**

12:30 p.m. **AADR Chapter Meeting**

KCRB AUDITORIUM

NO FOOD OR DRINKS
ALLOWED IN AUDITORIUM

Welcome from the Deans

Ron Sakaguchi, D.D.S., Ph.D., M.B.A.
DEAN, OHSU SCHOOL OF DENTISTRY

Hui Wu, Ph.D.
ASSOCIATE DEAN, OHSU SOD RESEARCH

Special Guests

Barry Taylor, D.M.D., CAE
EXECUTIVE DIRECTOR, OREGON DENTAL ASSOCIATION

Cyrus Lee, D.M.D.; Dan Pihlstrom, D.D.S.
PERMANENTE DENTAL ASSOCIATES

Ray Cohlmia, D.D.S.
EXECUTIVE DIRECTOR / CHIEF OPERATING OFFICER,
AMERICAN DENTAL ASSOCIATION

Keynote Speaker

"The Emerging Technologies that will Shape the Future of Dentistry"

Wenyuan Shi, Ph.D.
PRESIDENT AND CHIEF EXECUTIVE OFFICER, FORSYTH INSTITUTE

Best Poster Awards

3:00 p.m. **End of Research Day 2023**



ADA C-E-R-P® | Continuing Education
Recognition Program

SCHOOL OF DENTISTRY



"The Emerging Technologies that will Shape the Future of Dentistry"

by **Wenyuan Shi, Ph.D.**

President and Chief Executive Officer
Forsyth Institute

Thursday, March 2, 2023 | 12:30 p.m.

**Knight Cancer Research Building (KCRB) Auditorium
2720 S.W. Moody Ave.
Portland, OR 97201**

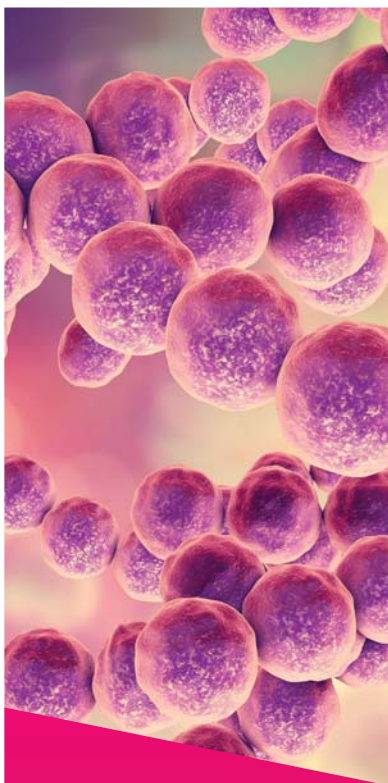
For more information about the speaker series, please call **503-494-7576** or visit **www.ohsu.edu/school-of-dentistry/sod-research-day**. Please note it takes about 20 minutes to travel to RLSB from Marquam Hill locations.



ADA CERP® | Continuing Education
Recognition Program

OHSU School of Dentistry is an ADA CERP Recognized Provider. ADA CERP is a service of the American Dental Association to assist dental professionals in identifying quality providers of continuing dental education. ADA CERP does not approve or endorse individual courses or instructors, nor does it imply acceptance of credit hours by boards of dentistry.





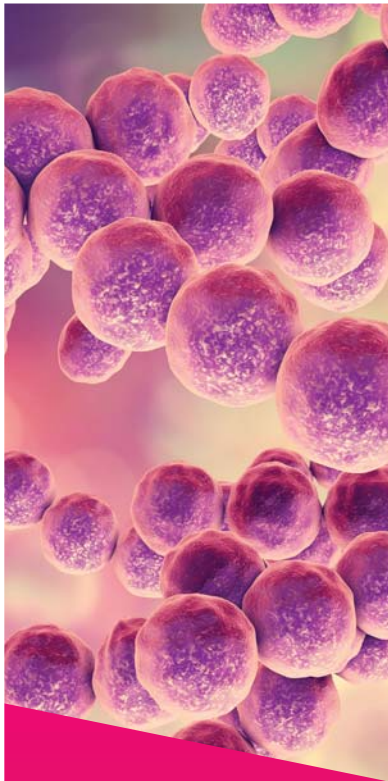
2023 Research Day

POSTER SESSION #1 - 8:30-9:30am

KCRB MAIN LEVEL

Poster Session #1 (Alphabetical by Presenter's last name)			
Poster-board #	Presenter(s):	Category:	Title:
26	David Anderson	Staff	Structural Investigations of the RNA Degradosome by Electron Microscopy
24	Robby Bergstrom, DS2	CaseCAT	Adverse Childhood Experiences and Healthcare Utilization
5	Christina Borland	Staff	Comparative Genomics Reveals Insight into Streptococcus anginosus Invasive Disease
1	Bryce Bothwell, DS3	DMD Student	Autonomic Nervous System (ANS) Activity and Longitudinal Temporomandibular Joint (TMJ) Health
14	Aaron Compton	Resident	Aggressive management of recurrent peripheral ossifying fibroma in the esthetic zone.
13	Juliana da Fonte	PostDoc	An analysis of the effects of orthognathic surgery on TMJ surface congruency
6	Emily Helliwell	Staff	Biogenesis and Characterization of Extracellular Membrane Vesicles from Streptococcus sanguinis
7	Dustin Higashi	Staff	Studies on Parvimonas micra-Neutrophil interactions reveal insights into the pathogenesis of this oral pathobiont.
12	Madeline Krieger*	PostDoc	Fusobacterium nucleatum Subspecies Exhibit Oral Niche-Specific Biases
19	Peter Lahti, DS3	CaseCAT	The impact of maxillary skeletal expansion on objective measures of nasal resistance in adults and children.
15	Chelsea Mansfield	Resident	The effect of surface topography after piezoelectric root-end resection on confidence level of detection of apical microcracks
20	Tyler McCreddie and Austin Gorton, DS1s	CaseCAT	The Ortho Endo Paradox: Can endodontically teeth move like their vital counterparts?
3	Zoie Newman	Staff	A 5-Year Analysis of Patient Complaints in the OHSU Dental Clinics
25	Luke Nordlie, DS3	DMD Student	Long-term performance of single unit implant-supported ceramic restorations using a fully digital workflow at the OHSU predoctoral clinic: a retrospective clinical study
9	Hua Qin	Staff	Analysis of protein-protein interaction by split luciferase complementation assay in Streptococcus mutans
16	Abasin Safi	Resident	Penetration of two bioceramic sealers into lateral canals of curved canals obturated with a single-cone gutta percha technique
17	Amy Schlehofer	Resident	alloOss Plus Case Report
21	Stella Sonu, DS3	CaseCAT	Evaluation of clinical effectiveness of Hall Technique for carious primary molars
27	June Treerat	Staff	Never judge a book by its cover: The mysterious case of Corynebacterium sp. isolation
22	Valerie Truong, DS1	CaseCAT	What is the role of dentists in treating pediatric obstructive sleep apnea?
23	Sarah Wiskoski, Luke George, and Grayson Wong, DS1s	CaseCAT	Clinical Reduction of Bisphenol-A leaching in dental restorations on younger patients
18	Hyun Yoon	Resident	Diagnostic agreement between an in-person and teledentistry visit within an academic health care setting during the COVID-19 pandemic
11	Zhengzhong Zou	Staff	Investigate the connection between cell death and natural competence development

*denotes PORT (Portland Oral Health Research Training) T90/R90 trainee



2023 Research Day

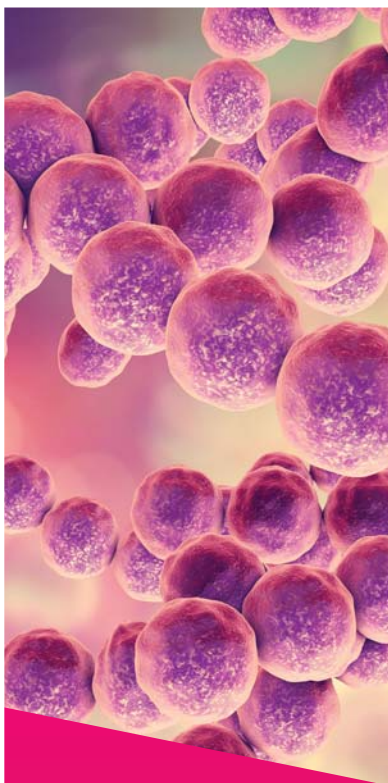
POSTER SESSION #2 - 9:40-10:40am

KCRB MAIN LEVEL

Poster Session #2 (Alphabetical by Presenter's last name)

Poster-board #	Presenter(s):	Category:	Title:
17	Bryce Bothwell, DS3	CaseCAT	Treatment and prevention of oral mucositis in adult patients undergoing chemotherapy treatment for leukemia
5	Juliana da Fonte	PostDoc	Does stitching mode influence the generation of beam hardening artifacts?
6	Genine Guimaraes	PhD Student	Antibacterial Effect Is Linked to Charge Concentration in Dimethacrylate Networks
10	Bao Huynh	Staff	An enzyme-responsive nanoplatform for preventing collagen degradation in dental tissues
16	Kiyono (Kay) Koi (Yamashita)	Faculty	The color matching ability of single-shade composites
11	Steven Lewis	Staff	Stress and Gel-Point Conversion in Disulfide and Thiol-Modified Dental Resins
15	Matthew Logan	Faculty	Exploring GtfC Inhibition via a Fluorescent Sugar Assay
8	Fernanda Lucena*	PostDoc	CHX or DOX-loaded TiO ₂ -nanotubes adhesives as anti-MMP strategy
12	Luke Miller	Staff	Design and validation of a co-polymerizable MMP inhibitor
18	Jonathan Nguyen, DS1	CaseCAT	Effective treatment of pediatric alveolar cleft lip and palate with rhBMP-2 bone graft
19	Luke Nordlie, DS3	CaseCAT	Robotic Systems in Implantology: Are they viable?
4	Clara Park, DS2	DMD Student	Thiol Content Determination of Thiourethane Functionalized Fillers for Dental Composites
20	Sehoon Park and Riley Smart, DS1s	CaseCAT	Which adhesive is more effective for treating non-cariou cervical lesions?
13	Sarah Patty	Staff	Carboxybetaine-based switching molecule to attack/defend against bacteria
9	Sivashankari Rajasekaran	PostDoc	Influence of synthesis parameters on the structure and stability of poly(urea-formaldehyde) microcapsules
21	Merit Roshdy, DS3	CaseCAT	Conventional Vs. Immediate Loading of Fixed Dentures in Edentulous Jaws
3	Noor Saeed, DS1	DMD Student	Does salivary pellicle affect the antibacterial efficacy of QAM-based composite?
22	Annelise Shaw, DS2	CaseCAT	Partially vs fully guided dental implant surgery
1	Chris Steiner	DMD Student	Dental Student Provision of Tobacco Cessation Advice and Assistance
23	Tiffany Tep, DS2	CaseCAT	Assessing dental competency in the recognition and diagnosis of orofacial pain
7	Fernanda Tsuzuki	PhD Student	Mechanical properties, bond strength and surface characterization of 3Y-TZP after different surface treatments protocols
14	Samuel Weber	Staff	Bond Strength and Polymerization Kinetics Study of Acrylamide Adhesive Formulations
2	Sarah Wiskoski	DMD Student	Filler Size Effects Surface Properties of Composites Pre-/Post-Toothbrush Abrasion

*denotes PORT (Portland Oral Health Research Training) T90/R90 trainee



2023 Research Day

POSTER SESSION #3 - 10:50-11:50am

KCRB MAIN LEVEL

Poster Session #3 (Alphabetical by Presenter's last name)			
Poster-board #:	Presenter(s):	Category:	Title:
13	Avathamsa Athirasala*	PostDoc	A bone metastasis on-a-chip approach to study the preferential growth of cancer cells into bone
9	Anissa Bartolome	Staff	RegendoGEL: A novel tooth-derived hydrogel for pulp & dentin regeneration
16	Andrea Bornstein, DS3	CaseCAT	Impostor Phenomenon in Dental Students
17	Ahmed Elamin, DS3	CaseCAT	Not all therapies are created equal: The effectiveness of Amoxicillin and Metronidazole adjunctive periodontal therapy on clinical outcomes in diabetic patients with periodontitis compared to SRP only or in combination with other adjunct Periodontal therapy medications
6	Cristiane Franca	Faculty	Perivascular cells mediate collagen stiffness and architecture sensing in blood vessels
8	Haylie Helms*	PhD Student	Single Cell Bioprinted Cell Circuits for the Systematic Assessment of Cell-Cell Communication in the Early Tumor Microenvironment
5	Ginny Ching-Yun Hsu	Faculty	Differential pericyte marker expression in craniofacial benign and malignant vascular tumors
18	Angela Hung and Whitney Warth, DS1s	CaseCAT	Clinical Outcomes of Delayed & Immediate Dental Implant Placement
19	Anthony Kerr, DS2	CaseCAT	Assessing Quality of Life for Patients with Trigeminal Neuralgia
2	Kirsten Lampi	Faculty	The building blocks of eye lens beta-crystallins are hetero-dimers
20	Isaac Lee, DS2	CaseCAT	The Effects of Laser Therapy in Periodontal Disease
14	Rahul Madathiparambil Visalakshan	PostDoc	Faster biomineralization and osteogenesis on-a-chip using 3D bioprinting and microfluidics
12	Stephanie Momeni	PostDoc	Butyrolactone-Ladderane Biosynthetic Gene Cluster Influences Streptococcus mutans Cariogenic Factors
11	Rong Mu	Staff	Plasmalogen, a glycerophospholipid crucial for S. mutans acid tolerance and colonization
1	Sylvia Nelsen	Faculty	Integrating Dental Gross Anatomy and Flipping it on its Head
7	Jonathan Nguyen, DS1	DMD Student	Investigating the Effects of Microfluidic Technology on the Biomineralization of Collagen Scaffolds in Bone-on-a-Chip.
10	Narendra Singh	Staff	Laser based-bioprinting of large 3D heterogenous tissues with vascular networks using poly(N-isopropylacrylamide) as sacrificial templates
15	Mauricio Sousa*	PostDoc	Development of a bone-like microenvironment on-a-chip to simulate osteoclastogenesis
22	Raesah Taher, DS3	CaseCAT	Antimicrobial Efficacy of Amnion Chorion Membranes Versus Platelet-Rich Fibrin
23	Ali Saad and Valerie Thai, DS2	CaseCAT	End to edentulism: Anti-USAG-1 Therapy for tooth regeneration
3	Baotong Xie	Faculty	The role of the gene polychaetoid in aging
4	Hua Zhang	Faculty	Structural and functional insight into biofilm regulatory protein in Streptococcus mutans

*denotes PORT (Portland Oral Health Research Training) T90/R90 trainee

SCHOOL OF DENTISTRY



Research Day

THURSDAY, MARCH 2

KCRB

RESEARCH PRESENTATION ABSTRACTS



ADA C-E-R-P® | Continuing Education Recognition Program

Structural Investigations of the RNA Degradosome by Electron Microscopy

David Anderson

Senior Research Associate, Merritt lab, Dept of Restorative Dentistry, OHSU School of Dentistry

Co-Author: Justin Merritt, Ph.D., OHSU School of Dentistry

Introduction:

The RNA degradosome is a multicomponent machine that uses ribonuclease activity to globally regulate host cell transcript abundance. Two RNases (J1 and J2) drive this machine in *Streptococcus mutans*, a leading cause of dental caries. We seek to test the hypothesis that an efficient cellular strategy to respond to dynamic environmental conditions would be to tune the activity of host cell machinery via association with a diverse array of proteins. Accessory components would direct the transcript targeting profile by means of allostery or inhibition, providing a direct link between metabolic status and posttranscriptional regulation at minimal energy cost to the cell.

Methods:

Our strategy to define the architecture of the degradosome is to combine single-particle cryo-electron microscopy with chromosomally-expressed RNase J2 fused to a cleavable epitope tag. This allows for a native level of expression and an unbiased association with the cellular milieu. Immunopurified complexes are proteolytically released into the supernatant and directly applied to grids for negative staining or vitrification.

Results:

Negative staining results revealed that classification of these particles may be possible for high resolution single particle microscopy. Two major classes of particles were evident in 3D volumetric reconstructions, each of which appear to be able to accommodate at least 3 additional proteins identified by mass spectrometry.

Conclusions:

If successful, we believe this approach will set a framework to study other protein systems to reveal the structural organization of unprecedented cellular complexes.

Comparative Genomics Reveals Insight into Streptococcus anginosus Invasive Disease

Christina Borland

Research Associate, Kreth lab, Dept of Oral Rehabilitation and Biosciences, OHSU School of Dentistry

Co-Authors: Yasser M. AbdelRahman and Justin Merritt

Introduction:

Although Streptococcus anginosus group bacteria are a normal part of the human oral microbiome, they are also associated with a wide range of infections, from dental abscesses to septicemia. The direct mechanisms by which these commensal bacteria become invasive are unclear. One possibility is that poor oral hygiene results in environmental conditions that facilitate invasion regardless of the specific genotype of the commensal strain; another is that certain genotypes are more likely to take advantage of environmental opportunities to become invasive.

Methods:

Whole genome alignments of sequenced isolates were used to identify synteny groups as well as core genes for phylogenetic analysis. Genome-Wide-Association-Studies (GWAS) was used to identify candidate loci for the invasive index. Polymerase chain reaction (PCR) analysis of strains found in the blood of septic patients confirmed the presence or absence of loci in clinical isolates.

Results:

792 core genes and six types of core synteny were identified from 74 sequenced isolates of Streptococcus anginosus. Phylogenetic analysis identified a new distinct cluster of 31 strains, predominantly isolated from healthy urogenital tract. The remaining 43 strains contained eight invasive strains isolated from bacteremic patient blood samples. These invasive strains did not fall into a single phylogenetic cluster, but were biased towards one specific clade. GWAS identified key loci allowing us to develop a PCR-based invasive index, the utility of which was confirmed by screening 37 additional clinical isolates from the blood of septic patients.

Conclusions:

These data suggest that certain genotypes of S. anginosus are more likely to become invasive given the opportunity. A PCR-based invasive index can be used to identify such strains.

Autonomic Nervous System (ANS) Activity and Longitudinal Temporomandibular Joint (TMJ) Health

Bryce Bothwell

DMD Student, OHSU School of Dentistry

Mentors: Jeff Nickel, Laura Iwasaki

Introduction:

Heart rate variability (HRV) is the change in time interval between consecutive heart beats. High HRV is associated with people of younger age and higher parasympathetic nervous system activity. Low HRV is associated with subclinical stress and chronic diseases, and higher tonic (continual low-level) sympathetic nervous system activity. Sympathetic nervous system activity is associated with increased jaw muscle activity, theoretically resulting in increased TMJ loading. Thus, increased tonic sympathetic nervous system activity may promote fatigue of the TMJ articulating tissues, leading to degenerative joint disease and TMJ-related pain. This pilot project measured nocturnal ANS activity in humans to determine if this was related to longitudinal changes in TMJ architecture.

Methods:

All subjects consented to participate according to OHSU IRB oversight. Cone-beam computed tomography and magnetic resonance imaging of subjects' TMJs were completed and interpreted by a calibrated radiologist initially (T1) and at follow-up (T2) ≥ 5 years later. TMJs were grouped according to T1-T2 changes, where Group A showed no change, Group B showed improved anatomy (amelioration of disc displacement or degenerative joint disease), and Group C showed regression (worsening of disc displacement or degenerative joint disease). Subjects were trained to use portable electrocardiographic recorders and asked to provide 3 night-time recordings, each >6 hours in duration. HRV was analyzed using commercial software (MindWare Technologies Ltd.) to quantify ANS activity during sleep. Time and frequency domain measures were determined from night-time electrocardiographic recordings. Recording statistics were then analyzed using Student T Tests and effect size measures to determine if there were statistically and clinically significant differences in night-time ANS activities between Groups B and C.

Results:

Ten subjects, five each in Groups B and C completed participation, where average T1-T2 interval was ≥ 5 years. A completed analysis of electrocardiographic recordings and the relationship between ANS activity and changes in TMJ architecture will be completed and data presented.

Conclusions:

Conclusions will be finalized following completion of HRV analyses.

Aggressive management of recurrent peripheral ossifying fibroma in the esthetic zone

Aaron Compton

Resident, Periodontology, OHSU School of Dentistry

Mentor: Dr. Yota Stahopoulou

Co-Authors: Dave Chandra, OHSU Pathology

Introduction:

Numerous reactive lesions presenting with gingival overgrowth include pyogenic granuloma, peripheral giant cell granuloma, and peripheral ossifying fibroma (POF). POF is a common gingival growth which originates from the periodontal ligament and can be associated with local irritants (plaque, calculus, subgingival restoration). POF, as well as other reactive gingival lesions, presents as a sessile or pedunculated lesion which is usually ulcerated and erythematous. Recurrence of POF is considered high ranging from 16-20%. The aim of this case report is to demonstrate the importance of proper diagnosis and aggressive treatment to prevent recurrence.

Methods:

A healthy 55yo Hispanic female presented to OHSU Grad Perio with a painful (8/10), slow growing mass on the facial gingival margin of #9. The lesion measures 12x12x6mm and is firm, immobile, ulcerated, erythematous, slightly pedunculated lesion. According to the patient, the lesion has persisted for 18 years with 10 excisions by different providers (recurring every 1-1.5 years). Patient reports the mass becoming larger with recurrence. The lesion was referred to grad perio for “esthetic management” of the recurrent lesion.

Results:

Full thickness soft tissue excision performed with 2mm margins including the central maxillary papilla. Osseous defect noted #9 facial with hemorrhage originating from #9 mesiofacial PDL space. Ostectomy performed and curettage of PDL space with round burs, hand instruments, and flame finishing burs to gain access to PDL space and remove hemorrhagic soft tissue component. SRP and occlusal adjustment performed. Biopsy sent for histology by OHSU pathology. Histopathology is consistent with developing peripheral ossifying fibroma. With 7 month follow up, no recurrence and complete resolution of symptoms noted. Esthetics are acceptable to patient with slight recession noted on #9.

Conclusions:

Proper diagnosis and treatment is necessary to prevent recurrent gingival reactive lesions. Lesions with a history of recurrence and conservative management should be treated with more aggressive curettage to prevent recurrence.

An analysis of the effects of orthognathic surgery on TMJ surface congruency

Juliana da Fonte

PostDoctoral Fellow, OHSU School of Dentistry

Co-Authors: Laura Iwasaki; Daniel Leo; Jeff Nickel

Introduction:

Orthognathic surgery is a widely used procedure to correct maxillofacial deformities. In the United States, maxillofacial discrepancies afflict 5% of the population and approximately 10,000 procedures are performed annually. However, loss of structural integrity of the condyles is a common complication following orthognathic surgery. Therefore, this study aims to evaluate the effects of orthognathic surgery on surface conformation and TMJ contact mechanics by comparing pre-and postsurgical CBCT scans using voxel-based superimposition methods, volumetric segmentation, and finite element analysis.

Methods:

CBCT scans used in this study are from 45 patients seen at Oregon Health & Science University, School of Dentistry, between January 2012 and January 2022, who underwent orthognathic surgery (sagittal osteotomy of the mandibular branches and Le Fort I) performed by the same team of oral and maxillofacial surgeons, and who have CBCT scans performed before and approximately 1 month after surgery. The selected CBCT images were exported in DICOM and coded in pairs to compare before and after orthognathic surgery of the same patient (A1-A2; B1-B2;). From the already selected pre- and postoperative DICOM files, segmentation of the mandibular head and temporal bone on both sides of each sample is performed using Amira Software®. Then, the segmented TMJ volumes will be rendered and superimposed using COMSOL Multiphysics® software and using finite elements, the following will be performed: I) measurement of changes in congruence of the surfaces of the mandible head and temporal bone as a result of the x, y, z rotation of the proximal segment, and II) identification of the pre-and postoperative limits, assessing the mechanical stress based on Hertzian contact mechanics.

Results:

A completed analysis of the segmentation of the condyles and temporal bones on both sides in 10 samples, using Amira Software®, and the measurement of the changes in the congruence of the surfaces of the mandibular head and temporal bone, using finite elements, will be completed and data presented.

Conclusions:

The conclusions will be finalized after the segmentation analyses are completed.

Biogenesis and Characterization of Extracellular Membrane Vesicles from *Streptococcus sanguinis*

Emily Helliwell

Senior Research Associate, Kreth lab, Dept of Oral Rehabilitation and Biosciences, OHSU School of Dentistry

Co-Authors: Dongseok Choi, School of Public Health, Oregon Health & Science University

Justin Merritt, Dept of Oral Rehabilitation and Biosciences, OHSU School of Dentistry

Jens Kreth, Dept of Oral Rehabilitation and Biosciences, OHSU School of Dentistry

Introduction:

Streptococcus sanguinis is prevalent in the oral cavity and inhibits colonization of oral pathogens. Like other cell types, streptococci produce extracellular membrane vesicles, which contain specific molecular cargo and interact with host cells. Our goal is to establish the environmental and community conditions that play a role in *S. sanguinis* vesicle production, and to characterize the immunostimulatory effects of vesicles on eukaryotic cells.

Methods:

We used differential centrifugation methods coupled with image analysis to isolate and quantify *S. sanguinis* vesicles. Transcriptomic analyses combined differential expression and correlation of count data with vesicle quantity to examine gene expression changes underlying vesicle production. Proteomic characterization of the vesicle cargo was done via mass spectrometry. To test the immunostimulatory effects, *S. sanguinis* vesicles were inoculated onto gingival epithelial cells, followed by gene expression analysis.

Results:

Vesicle production is dependent on both environmental and community factors; carbohydrates differentially affect vesicle production with more than an 80% reduction in vesicle number in cultures supplemented with sucrose as compared to glucose. Co-culture with interacting commensal *Corynebacterium durum*, as well as with pathobiont *Filifactor alocis* had no effect on *S. sanguinis* vesicle number, whereas pathobiont *Porphyromonas gingivalis* greatly reduced *S. sanguinis* vesicle number. Expression of genes encoding proteins localized to the cytoplasmic membrane correlate with the abundance of vesicles. Proteomic characterization of the vesicle cargo identified several proteins predicted to influence host immune responses. Studies of gingival epithelial cells demonstrated that vesicles induced the expression of IL-8, TNF- α , and Gro- α without causing cell death.

Conclusions:

S. sanguinis vesicle production is influenced by community and environmental factors, and plays a role in communication with host cells. The immunostimulatory effects of *S. sanguinis* vesicles highlight an important role in commensalism; in which a microbe induces an immune response but avoids damage to host cells, thus discouraging infection by pathobionts.

Studies on *Parvimonas micra*-Neutrophil interactions reveal insights into the pathogenesis of this oral pathobiont.

Dustin Higashi

Research Associate, Merritt lab, Dept of Oral Rehabilitation and Biosciences, OHSU School of Dentistry

Co-Authors: Dustin L. Higashi¹, Zhengzhong Zou¹, Hua Qin¹, David Anderson¹, Madeline C. Krieger¹, Lena Li¹, Christina Borland¹, Elizabeth A. Palmer², Jens Kreth^{1,3}, and Justin Merritt^{1,3*}

¹Department of Restorative Dentistry

²Department of Pediatric Dentistry

³Department of Molecular Microbiology and Immunology

Introduction:

Parvimonas micra is a pathobiont from the oral cavity that is strongly associated with mucosal dysbiotic disease, as well as multiple types of cancer. Inflammation is a hallmark of a number of oral diseases such as periodontitis and apical abscesses, and corresponds to an influx of neutrophils (PMNs) to sites of infection. PMNs play a major role in the clearance of pathogenic microbes as well in immune system homeostasis. Despite the presence of PMNs at sites of these oral diseases, *P. micra* levels are actually enriched. We hypothesize that *P. micra* have evolved the ability to circumvent destruction by PMNs.

Methods:

PMNs were isolated from the peripheral blood of human subjects and in vitro infection studies with *P. micra* were performed. We determined PMN phagocytic capacity using high-resolution microscopy as well as gentamicin protection assays. We further investigated the PMN response to *P. micra* exposure using flow cytometry to measure viability and degranulation and determined bacteria survival using plating assays.

Results:

P. micra is efficiently phagocytized by PMNs and do not significantly induce apoptosis or degranulation. *P. micra* is able to survive intracellularly and extracellularly among PMNs.

Conclusions:

Successful pathogens have the ability to overcome host defenses to cause disease. The ability of *P. micra* to survive killing by PMNs at sites of active PMN influx and abundance, may reflect its success in establishing infections. Studies exploring the nature of *P. micra*-PMN interactions will allow for a better understanding of the development of inflammatory diseases such as periodontitis and endodontic abscesses.

Fusobacterium nucleatum Subspecies Exhibit Oral Niche-Specific Biases

Madeline Krieger

PostDoctoral Fellow / PORT T90 Trainee*, Merritt lab, Department of Oral Rehabilitation and Biosciences,
OHSU School of Dentistry

Co-Authors: Yasser AbdelRahman, Justin Merritt, Elizabeth Palmer

Introduction:

Fusobacterium nucleatum, a ubiquitous member of the human oral and gut microbiomes, is strongly associated with the development of multiple human diseases including periodontitis, oral/extraoral abscesses, and several types of cancer. *F. nucleatum* is currently divided into four subspecies: *F. nucleatum* subspecies *nucleatum* (*Fn. nucleatum*), *animalis* (*Fn. animalis*), *polymorphum* (*Fn. polymorphum*), and *vincentii/fusifforme* (*Fn. vincentii*). Although these subspecies have been historically considered as functionally interchangeable, recent clinical studies of colorectal tumor-associated *F. nucleatum* have suggested this perception may be inaccurate. Consequently, we aimed to determine whether *F. nucleatum* subspecies prevalence in the oral cavity correlates with oral health status.

Methods:

Patient-matched specimens of dental plaque and odontogenic abscess were analyzed with both culture-independent and culture-dependent approaches using 58 and 44 paired samples, respectively. Pangenome, phylogenetic and functional enrichment analysis of *Fusobacterium* species and *F. nucleatum* subspecies were conducted using the Anvi'o workflow.

Results:

Both culture-independent and -dependent analyses similarly revealed a highly biased distribution of *F. nucleatum* subspecies in the oral cavity, with most patients harboring multiple subspecies. In dental plaque, *Fn. polymorphum* is the dominant organism, whereas *Fn. animalis* is particularly prevalent within abscesses. Surprisingly, the most heavily studied subspecies, *Fn. nucleatum*, was only a minor constituent within the entire specimen collection. In agreement with the clinical data, phylogenetic and comparative genomic analyses identified substantial distinctions among *F. nucleatum* subspecies.

Conclusions:

The heterogeneous distribution of *F. nucleatum* subspecies within oral plaque and abscess specimens reveals niche-specific preferences, with *Fn. animalis* likely exhibiting the greatest pathogenic potential. Both the clinical and genomic data strongly suggest that each *F. nucleatum* subspecies likely comprises unique *Fusobacterium* species.

**PORT (Portland Oral Health Research Training) T90/R90 Program is an OHSU School of Dentistry training program, funded by NIH/NIDCR, that supports mentored training in oral and craniofacial health research to PreDoctoral, Dual Degree, PostDoctoral, and Foreign-Trained Dentist trainees.*

The effect of surface topography after piezoelectric root-end resection on confidence level of detection of apical microcracks

Chelsea Mansfield

Resident, Division of Endodontics, OHSU School of Dentistry

Co-Authors: Dr. Karan Replogle

Introduction:

Piezoelectric devices atraumatically cut hard tissue using controlled ultrasonic vibrations. They are used in endodontic microsurgery for osteotomy, root-end resection and root-end preparation. This in vitro study investigates the effect of root-end surface topography created by piezoelectric activity compared to conventional carbide bur resection on the confidence level of detecting apical microcracks.

Methods:

Thirty bilaterally matched pairs of single-rooted human teeth were divided into two study groups: piezoelectric and multipurpose. Resections were timed and performed 3mm from the apex using a Piezosurgery® diamond-coated OTA1 insert or a high-speed multipurpose carbide bur. A Zumax® surgical operating microscope at 20x magnification captured images of the root ends in three different conditions: unstained, stained (methylene blue), and stained plus transillumination. Two independent, blinded observers viewed the randomized images and rated surface topography as well as confidence level regarding ability to detect microcracks under the three different conditions. Agreement in observer confidence level, surface roughness ratings, and resection time were analyzed.

Results:

Observers were less confident in assessing for microcracks in root-end resections made in the piezoelectric group. Confidence levels increased in both groups after staining plus transillumination. Surface roughness ratings were highest in the piezoelectric group with confidence decreasing as roughness rates increased. Resection times in the piezoelectric group were 3 times longer than the multipurpose group.

Conclusions:

Rough surface topography of piezoelectric root-end resection decreased confidence in the detection of apical microcracks.

A 5-Year Analysis of Patient Complaints in the OHSU Dental Clinics

Zoie Newman

Quality Improvement and Patient Relations Program Manager, Office of Clinical Systems,
OHSU School of Dentistry

Co-Authors: Dr. Despoina Bompolaki

Introduction:

As patients become more aware of their rights, the rates of submitted complaints in healthcare environments has been increasing over the last decades. The collection and resolution of such complaints is a significant area for quality improvement. The purpose of this study was to analyze the prevalence and type of patient complaints that were filed in the OHSU SOD Dental Clinics during a 5-year period (2017-2022). A secondary purpose was to determine whether specific patient and/or provider characteristics were associated with patient complaints.

Methods:

A retrospective review of patient complaints reported to the OHSU SOD Patient Advocate from 2017 to 2022 was conducted. All complaints were registered by the OHSU SoD Patient Advocate, as part of the routine Quality Improvement process. All complaints from patients with an individual electronic health record were included in the analysis. Patients who did not complete the patient registration process to create an electronic health record were excluded. Complaints filed by parents or guardians of minors were excluded. The specific information that was extracted for each registered complaint included: Year when complaint was registered; Patient gender and age; Provider gender; Provider type (faculty/resident/student); Category of complaint (Billing/Communication/Behavior/Clinical Treatment/Scheduling). Data analysis was completed using a statistical analysis software program (IBM SPSS Statistics, v28; IBM Corp). Odds ratios were calculated to detect differences in gender among those patients who filed a complaint. Chi-square tests were used to detect differences in the patient gender for complaints that were filed against a female vs. a male provider. The level of significance was set to $\alpha = 0.05$.

Results:

The data analysis for this study is currently being finalized. Our results so far indicate that the majority (44.6%) of filed complaints during the study period were related to clinical treatment. A significant percentage (44.8%) of complaints resulted from unideal interpersonal interactions, more specifically related to behavioral (23.5%) or communication (21.3%) issues. Male providers received more complaints than female providers. However, chi-square tests did not reveal a significant correlation between patient gender and provider gender ($p = .617$). Odds ratios did not reveal a significant difference on whether a complaint was filed or not, in regard to patient gender ($z = 1.589, p = .11$).

Conclusions:

Having an in-depth understanding of the nature of patient complaints and the demographics of those who complain, provides invaluable insight not only to the providers but also to those who are involved in the grievance resolution process. Regular analysis of past and current trends related to patient grievances will not only improve the overall quality of the grievance resolution process but will also allow for overall process improvements in order to obtain greater patient satisfaction and ultimately improve dental care as a whole.

Long-term performance of single unit implant-supported ceramic restorations using a fully digital workflow at the OHSU predoctoral clinic: a retrospective clinical study

Luke Nordlie

DMD Student, OHSU School of Dentistry

Mentor: Despoina Bompolaki

Co-Authors: Peter Lahti, Despoina Bompolaki

Introduction:

The OHSU predoctoral program has used CAD/CAM ceramic implant-supported crowns using a fully digital workflow for over 6 years. Long-term clinical studies on the performance of these restorations are still limited. The purpose of this study was to provide clinical data on the performance of CAD/CAM ceramic implant-supported crowns that had been in function for at least 12 months. The type and rate of complications associated with this type of restorations as well as their overall success and survival rates were calculated. Additionally, this study aimed to identify any correlation between prosthesis survival/complication rate and any patient-related or clinical factors.

Methods:

IRB approval was obtained. All adult patients that received a CEREC implant-supported crown at the OHSU predoctoral clinic at least 12 months before the study's start date were identified. Electronic health records were thoroughly examined by 2 independent, calibrated examiners (L.N and P.L.). Any discrepancies in data entry were discussed among the study members until consensus was reached. Extracted data included type and date of complications that occurred until the patient's last visit at OHSU. Documentation of occlusal guard delivery after insertion of the implant-supported restoration was noted. Data analysis was completed using a statistical analysis software program (SPSS, version 25).

Results:

A total of 214 restorations were included in the study. The mean follow-up time was 2.5 years (range 1-4.75 years). Of the restorations included in the analysis, 87 (40.6%) presented with at least 1 complication during the follow-up period, for a success rate of 59.4%. Seven restorations (3.3%) presented with 3 or more complications. The most commonly reported complications were opening of the proximal contact and prosthetic screw loosening. A total of 11 (5.1%) restorations failed, yielding a restoration survival rate of 94.9%. The majority of patients (over 80%) did not receive an occlusal guard after the treatment was completed.

Conclusions:

Based on the results of this study, ceramic implant-supported crowns made with a fully digital workflow are expected to have a relatively high number of complications. However, the survival rates are high and comparable to restorations that are made using conventional workflows. Following best clinical practices can help reduce complications, but additional amounts of chair time should be expected to address prosthesis-related complications that may arise following delivery of the definitive restoration. Occlusal guards are recommended to all patients receiving implant-supported restorations.

Analysis of protein-protein interaction by split luciferase complementation assay in *Streptococcus mutans*

Hua Qin

Senior Research Associate, Department of Oral Rehabilitation and Biosciences, Merritt lab,
OHSU School of Dentistry

Co-Authors: David Anderson, Zhengzhong Zou, Dustin Higashi and Justin Merritt

Introduction:

Proteins are indispensable in all biological systems, and while many proteins perform their functions independently, the vast majority of proteins interact with others for proper biological activity. Characterizing protein-protein interactions is critical to understand protein function and the biology of the cell. The split luciferase complementation assay (SLCA), the amino-terminal and carboxyl-terminal fragments of Renilla luciferase are translationally fused to two interested proteins, respectively, two non-functional halves of luciferase were brought into close enough proximity through a specific protein-protein interaction to restore the functions of the enzyme and emit detectable light. In this study, we have successfully confirmed a series of MecA interacting proteins and their binding affinity using SLCA in *Streptococcus mutans*.

Methods:

Mass spectrometry analysis of MecA coimmunoprecipitates (Co-IP) was employed to identify candidate protein-protein interaction partners. Candidate interactions were further confirmed using split luciferase complementation assay (SLCA).

Results:

Two split sites of Renilla luciferase, 155-156 and 229-330, were tested for SLCA. Both sites are suitable for SLCA. Mass spectrometry analysis revealed that MecA interacts with multiple proteins, such as tRNA sulfurtransferase (ThiI), NADPH-dependent glutamate synthase (GltB) and class III stress response-related ATP-dependent Clp protease (ClpC), etc. SLCA not only confirmed these interactions, also the interaction affinity between MecA and its interaction proteins exhibited similar trends with Co-IP mass spectrometry enrichment. SLCA further confirmed the N-terminal of MecA is the substrate binding site since the luciferase signal of N-fused MecA dropped tremendously.

Conclusions:

SLCA is a repetitively, quantitatively and noninvasively method to detect protein-protein interaction in vivo, with high sensitivity and low background, it measures dynamic protein-protein interaction in real-time, and it requires limited experimental materials and instrumentation.

AlloOss Plus Case Report

Amy Schlehofer

Resident, Graduate Periodontics, OHSU School of Dentistry

Mentor: Dr. Yota Stathopoulou

Co-Authors: Aaron Compton (Graduate Periodontics Resident)

Abstract:

A maxillary anterior guided bone regeneration (GBR) procedure was performed in a severely deficient site using AlloOss Plus, a mesenchymal stem cell bone allograft. Results were documented via cone beam computed tomography (CBCT), periapical radiographs, and clinical photographs. CBCT evaluation was performed at 6 months post-surgery. Clinical evaluations were performed at time of GBR and at 1 week, 2 weeks, 6 weeks, and 8 months post-operative visits. The GBR resulted in 0.2mm vertical and 3.9mm horizontal ridge gain based on CBCT. Photographic and radiographic images confirm increase in bone volume. Implants placed (2-stage) at 8 months in sites #8 and #10 achieved primary stability of 25 Ncm and 15 Ncm, respectively. The histologic examination of hard tissue biopsies is being processed (data to be presented at future time.) Clinical findings suggest AlloOss Plus is effective in horizontal ridge augmentation in a severely compromised site.

Introduction:

While autogenous bone grafts are still the gold standard for regeneration, many individuals do not want to undergo two separate surgical sites. The next closest alternative is Bone Viable Matrix (BVM) products. These two options offer three important aspects of bone repair. These properties include: osteoconductive, osteoinductive, and osteogenic components. They also offer angiogenic-factors. A new type of BVM has been released to market called, AlloOss Plus. AlloOss Plus contains cells that allow for proliferation and differentiation at a more affordable cost compared to other options on the market. AlloOss Plus contains viable cancellous bone with endogenous bone forming cells, osteoblast, osteocytes, OPG, and mesenchymal stem cells (MSC.) AlloOss Plus contains more osteoblasts per surface area that promotes increased bone growth. AlloOss Plus is said to retain more endogenous growth factors such as BMP-2. BMP-2 aids in the osteoinductive process. This case report attempts to look at AlloOss Plus used in a clinical setting, specifically for a guided bone regenerative procedure for plans of future implant placement.

Case Presentation:

A 72-year-old female with noncontributory medical history presented to OHSU Graduate Periodontal Clinic for comprehensive evaluation. The patient had a history of facial trauma and presented with teeth missing at sites #9 and #10 with a Siebert 1 ridge deficiency. Tooth #8 presented with a chronic apical abscess and was recommended for extraction due to a hopeless prognosis. Extraction of #8 with site preservation was performed. The materials used were Maxxeus cortical mineralized/demineralized blend (allograft) with Zimmer Collagen tape. Four weeks later, the guided bone regeneration (GBR) was completed in preparation for an implant bridge #8-#10. The materials used were: AlloOss Plus (BVM) with RCM6 membrane. At 8 months, the site was re-entered for evaluation of ridge and for implants to be placed at #8 and #10.

Procedure

A CBCT was captured at the initial patient visit of site #8. The patient then underwent an atraumatic extraction and ridge preservation procedure with a flapless design. The materials used were Maxxeus cortical mineralized/demineralized blend (allograft) with Zimmer Collagen tape. The site was left to heal for 4 weeks. At 4 weeks, a CBCT was captured at site #8 and the site was re-entered for the guided

bone regeneration (GBR) procedure with AlloOss Plus. The incision design included sulcular incisions on the buccal of #4M to #13M, with a crestal incision over edentulous sites #8-10, and vertical incisions on #4M and #13M. Full thickness flap reflection was made on the buccal and palatal surfaces. Cortical perforations were made with a 1/2 round bur over the edentulous site. The RCM6 membrane (30mm x 40mm) was trimmed and tucked on palatal. AlloOss bone thawed according to manufacturer's instructions and adapted to the site. The membrane was then adapted on the buccal and stabilized with 5-0 glycolon sutures. 3-0 cytoplast sutures were used to place three horizontal mattress sutures and eight simple interrupted sutures. 5-0 chromic gut was used to place simple interrupted sutures to reapproximate vertical incisions. At seven months a CBCT was taken to evaluate the bone. The surgical site was re-entered at 8 months with trephine burs to gather a sample for histologic evaluation of vital bone where the planned implants were to be placed. Biopsies were placed in 10% Neutral Buffered Formalin, fully covered and placed in room temperature. After the biopsy, the implants were placed with a surgical guide at sites #8 and #10. The selected implants were: Nobel Parallel CC TiUltra 4.3x10mm for site #8 and 3.75x10mm for site #10. Cover screws were placed and the flap was sutured with primary closure.

Results:

Upon placement of implants, it was evaluated the superficial layer of osseous structure had a membranous film to it. This fibrous material can be appreciated in the clinical photographs. It is possible this appearance and texture could be due to the RCM6 membrane. The texture of the bone at site #10 was soft and superficial bone was sluffing away. The texture of the bone at site #8 was solid in nature and able to withstand the osteotomy preparation for implant placement. Overall, the bone had a "rebound" nature when placing the implants. Implants were torqued to 15Ncm. And cover screws were placed with primary soft tissue coverage.

Conclusions:

Mesenchymal stem cells incorporated into an allograft have been shown to be an effective material for guided bone regeneration in areas with moderate ridge resorption. A follow up histologic evaluation will be provided from this case. More studies need to be performed with AlloOss Plus as it is still considered a newer product.

Penetration of two bioceramic sealers into lateral canals of curved canals obturated with a single-cone gutta percha technique

Abasin Safi

Resident, Endodontology, OHSU School of Dentistry

Co-Authors: Sousa Melo S.L., Yoon H, Arad A, Replogle KJ

Introduction:

Single-cone obturation techniques have re-emerged. Critical to the success of this technique is sealer flow into complex root canal systems. Flow is an essential property that allows the sealer to fill these diverse systems, isthmuses, and lateral canals. In this study, 3-D printed models were developed with curved root canals, and lateral canals for evaluation of sealer penetration following obturation. The models were used to compare the penetration of AH Plus Bioceramic sealer (Dentsply Sirona, USA) and NeoSEALER Flo (Avalon Biomed, USA) into lateral canals of curved canals obturated with a single gutta percha cone.

Methods:

3-D split models with simulated curved, and lateral canals (diameter 0.2mm, depth 5.0mm) positioned bilaterally at 1mm, 3mm, 5mm, and 7mm from apex were designed (#30/.04, 23.0mm length) and printed from resin polymer (Autodesk, San Rafael, CA). Canals (curved, n=50) were obturated with either AH Plus Bioceramic™ (n=25) or NeoSEALER Flo™ (n=25) and a single cone gutta-percha. The level of sealer penetration into lateral canals was measured using ImageJ™.

Results:

The depth of penetration of the sealer was not significantly different between the two bioceramic sealers. Sealer penetration into apically positioned lateral canals (1mm) was significantly less than at other levels.

Conclusions:

Sealer penetration into simulated lateral canals was similar between AH Plus Bioceramic and NeoSEALER Flo. Sealer penetration was less in the apically positioned lateral canals.

Never judge a book by its cover: The mysterious case of *Corynebacterium* sp. Isolation

June Treerat

Senior Research Associate, Kreth lab, Dept of Oral Rehabilitation and Biosciences, OHSU School of Dentistry

Co-Authors: Brian McGuire², Elizabeth Palmer², Erin M. Dahl³, Lisa Karstens³, Justin Merritt, and Jens Kreth

2: Department of Pediatric Dentistry, OHSU

3: Department of Molecular Microbiology and Immunology, School of Medicine, OHSU

Introduction:

The oral microbiome, harboring over 700 bacterial species, engages in highly sophisticated ecological interactions for maintaining symbiosis. Oral commensals are constantly affected by diverse challenges, leading to inter- and intra-personal oral microbiome variations. Nonetheless, certain features, including niche-specific bacterial taxa, remain sufficiently stable across time and subjects. Of those 700 species, *Corynebacterium* sp., especially *C. durum* and *C. matruchotii*, are among the core commensals. So far, the extended human oral microbiome database (eHOMD) lists 28 oral *Corynebacterium* species with little to no comprehensive characterizations. Hence, this study aimed to establish several comprehensive strategies optimized for oral corynebacteria isolation and characterization.

Methods:

Saliva collection and strain isolation were first conducted. Genomic DNA isolation and PCR were then performed for screening prior to whole-genome sequencing, de novo assembly, annotation, and phylogenomic tree analysis. Phenotype analyses, such as biochemical tests, free fatty acid production, and the ability to induce *Streptococcus sanguinis* chain elongation, were performed.

Results:

Six new oral isolates selected on oral *Corynebacterium* optimized selection medium (OCM), revealed *C. durum*-specific phenotypes, including the ability to induce *Streptococcus sanguinis* chain elongation in co-culture, and free fatty acid secretion. Moreover, biochemical analysis of the 6 isolates evaluated by the commercially available API Coryne biochemical tests matched closer to that of the reference strain *C. durum* ATCC33822. However, whole-genome sequencing grouped the new isolates closer to *Actinomyces* species. Phylogenomic analysis further verified the close relationship of the six isolates to *Actinomyces* species. Both *Corynebacterium* and *Actinomyces* are suborders of the Actinobacteridae and related species.

Conclusions:

Our current study, thus, emphasized an importance of taking several comprehensive strategies into consideration when taxonomically identifying closely related microorganisms.

Diagnostic agreement between an in-person and teledentistry visit within an academic health care setting during the COVID-19 pandemic

Hyun Yoon

Resident, Division of Endodontology, OHSU School of Dentistry

Co-Authors: Dr. Karan J. Replogle and Dr. Dongseok Choi

Introduction:

The COVID-19 pandemic altered the routine delivery of endodontic care. In response, audio or video teledentistry visits were conducted as the first visit for all patients referred to the Graduate Endodontic Practice at Oregon Health and Science University (OHSU) School of Dentistry (SoD) from August 2020 through December 2021. Provisional diagnosis and prognosis were made at the conclusion of each teledentistry visit, and clinical diagnosis and prognosis were made during the in person visit. Purpose of this study was to evaluate the diagnostic agreement between teledentistry visits and the control condition (in-person visits).

Methods:

A retrospective axiUm® chart review was completed to capture data from Aug 1, 2020 to Dec 31, 2021. In addition to diagnosis and prognosis, information on patient age, gender, need for interpreter, visit modality, length of teledentistry visit, time passed between teledentistry and in-person visit, tooth type, radiographs, and payor type was collected. Data was statistically analyzed to determine agreement between the virtual visit diagnosis and prognosis with that of the in-person visit (control condition). Analysis of the association of the variables with the lack of agreement was also conducted.

Results:

Total of 687 teeth from 575 patient charts were reviewed. Agreement for pulpal and periradicular diagnosis was 80% and 68% respectively. Agreement for pulpal diagnosis was highest for diagnosis of “previously treated”. Agreement for periradicular diagnosis was highest for diagnosis of “normal apical tissue”. Endodontic, periodontal, and restorative prognosis agreement was 86%, 84%, and 84% respectively.

Conclusions:

Endodontic diagnosis and prognosis agreement between virtual and in-person visits showed high to moderate agreement suggesting that virtual visits are a viable option for initial endodontic visits.

Investigate the connection between cell death and natural competence development

Zhengzhong Zou

Senior Research Associate, Merritt lab, Department of Oral Rehabilitation and Biosciences,
OHSU School of Dentistry

Co-Author: Justin Merritt, Ph.D., OHSU School of Dentistry

Introduction:

Many bacterial species undergo programmed cell death (PCD) as part of a defined, regulated pathway. PCD has a key role in various processes such as stress response, development, genetic transformation and biofilm formation. Different forms and molecular mechanisms of PCD have been described in bacteria. Here, we have found that overexpression of the core competence regulators ComR/X in *Streptococcus mutans* could induce a potent suicide-like cell death through an unknown mechanism.

Methods:

ComR/X were overexpressed under the control of a xylose-inducible promoter. Suppressor mutations were sequenced by Pooled Super-High Throughput sequencing method. ComX interaction proteins were identified by co-immunoprecipitation and mass spectrometry.

Results:

We ruled out the possibility that colony growth was due to mutations that abolish ComR or ComX activity and isolated a 96-well plate of suppressor mutations that can grow under comR/X overexpression cell death conditions. Sequence analysis of 44 comR overexpression cell death suppressors genomes identified SNP (single-nucleotide polymorphism) in *irvR* (encodes LexA-like regulator), *rcrR* (encodes an MarR-like transcriptional regulator) and *comX*. Both *rcrR* and *irvR* were shown to regulate *S. mutans* competence development through *comX*, indicating comR induce cell death through comX. Surprisingly, Sequence analysis of 47 comX overexpression cell death suppressors genomes only identified 2 clones both harboring SNP in *rpoC* which encodes DNA-directed RNA polymerase subunit beta' that resistant to both comR and comX induced cell death after re-testing. Co-IP mass spectrometry analysis of the ComX interactome in cell death conditions identified multiple highly enriched natural competence proteins, including SsbB, DprA, ComYA, RadA, and RadC.

Conclusions:

The results of this study provide new insights into the cell death pathway during competence development. While the detailed regulatory mechanisms are still an active area of investigation, our data indicated that both ComX and several late competence proteins are involved in inducing cell death during *S. mutans* competence development.

Does stitching mode influence the generation of beam hardening artifacts?

Juliana da Fonte

PostDoctoral Fellow, OHSU School of Dentistry
(visiting scholar, University of Campinas, School of Dentistry, Brazil)

Mentor: Deborah Queiroz de Freitas (University of Campinas, School of Dentistry, Brazil)

Co-Authors: Rocharles Cavalcante Fontenele, University of Campinas, School of Dentistry, Brazil

Introduction:

Cone-Beam Computed Tomography (CBCT) is an important imaging exam in dentistry. Despite its benefits, it has some limitations such as the production of artifacts. Artifacts impair image quality and can hinder the diagnosis of many conditions. The positioning of the object in the field of view (FOV) can change the image quality. The amount of noise in the image is greater when an object is on the FOV periphery than when it is centrally located. Therefore, this study aimed to compare the expression of artifacts generated by high-atomic-number materials in CBCT images acquired in different acquisition modes (stitching and partial).

Methods:

Fifteen CBCT scans were acquired from an acrylic resin phantom containing cylinder pairs of five different materials (amalgam, cobalt-chromium, gutta-percha, titanium, or zirconia) positioned in the encounter zones of the stitching mode. Thus, for each material, a CBCT scan was acquired in stitching mode, another anterior partial, and finally a posterior partial. CBCT scans were acquired on a CS9000 3D device (Carestream Health Inc., Rochester, NY, USA) at 70 kV, 10 mA, and 0.2 mm voxel size. Artifact expression was evaluated by calculating the mean and standard deviation (SD) of the gray shades of 4 regions of interest positioned around the cylinders (anteriorly, posteriorly, internally, and externally). Multi-way ANOVA was performed to test the effect of the studied factors (acquisition mode, ROI, and material).

Results:

The acquisition mode significantly influenced the expression of the artifacts generated by zirconia and cobalt-chromium ($p < 0.05$). The stitching mode presented the highest mean and SD values in the anterior ROI for both materials. Differently, the stitching mode also presented the lowest values for the posterior ROI only for cobalt-chromium.

Conclusions:

The acquisition mode of CBCT images influenced the expression of artifacts generated by zirconia and cobalt-chromium materials only.

Antibacterial Effect Is Linked To Charge Concentration In Dimethacrylate Networks

Genine Guimaraes

Visiting PreDoctoral Student, Pfeifer lab, Dept of Biomaterials and Biomedical Sciences, OHSU School of Dentistry

Mentor: Carmem S Pfeifer

Co-Authors: Matthew Logan¹; Genine Moreira de Freitas Guimaraes^{1, 2}; Sarah Patty¹; Marcelo Icimoto³; Lincoln Pires Borges⁴; Steven Lewis¹; Adilson Yoshio Furuse²; Carmem Silva Pfeifer¹.

- 1: Division of Biomaterials and Biomechanics, OHSU School of Dentistry, Portland, Oregon, UNITED STATES;
2: Department of Operative Dentistry, Endodontics and Dental Materials, Bauru School of Dentistry, University of Sao Paulo, Bauru, São Paulo, BRAZIL;
3: Department of Biophysics, Federal University of São Paulo, Sao Paulo, BRAZIL;
4: Department of Dental Materials, University of Campnas, Piracicaba, Sao Paulo, BRAZIL

Introduction:

The biofilm inhibition mechanism of quaternary ammonium methacrylates (QAM) has not been completely elucidated. While it is known that the side chain length and charge concentration both directly correlate with antibiofilm activity, the objective of this study was to de-couple their contributions, either as polymerizable (methacrylated-MA) or untethered (non-MA) compounds. The hypothesis was that charge concentration via polymerization-induced phase separation (PIPS) will directly correlate with antibiofilm activity.

Methods:

The experimental design consisted of molecules with: 16 carbon-side chain (C16); C16 with positive charge (QA-C16); C16 with positive and negative charges (CTAC+/-); or 6-carbon side chain (C6) with positive charge (QAM-C6). These compounds were added at 0-control or 10 wt% to (BisGMA:TEGDMA-1:1) resins, using 2,2-Dimethoxy-2 phenylacetophenone/Diphenyliodonium hexafluorophosphate (0.2/0.4 wt%) and butyl hydroxytoluene (0.1 wt%) as initiators/inhibitor. Polymerization kinetics in near-IR and light transmission in the UV-Vis range (320-500 nm, 35 mW/cm) through 0.8 mm specimens were assessed simultaneously in realtime using an optical bench apparatus. Light transmission reduction was used as a measure of PIPS in crosslinked networks. *S. mutans* biofilms on the surface of kinetics specimens were stained with crystal violet. Data were analyzed with one-way ANOVA/Tukey's test ($\alpha=5\%$).

Results:

Results show that DC was similar for all groups tested (~70%, $p=0.850$). QA-C6-MA and QA-C-16 showed the highest R, statistically different from the control ($p=0.000$). QA-C16 had the greatest light transmission reduction in all wavelengths, followed by QA-C6, all statistically higher than the control ($p=0.000$). QA-C16, C16 and CTAC+/- groups showed no biofilm on the surface.

Conclusions:

The highest biofilm inhibition in this study was observed with the long-chain, charged materials, which also showed the greatest reduction in light transmission. Although there was phase-separation with QA-C6, there was likely not enough charge concentration to prevent biofilm formation. Future studies will use fluorescein assay to determine charge concentration, and confirm this hypothesis.

An enzyme-responsive nanoplatform for preventing collagen degradation in dental tissues

Bao Huynh

Research Assistant, Fugolin lab, Division of Biomaterials & Biomechanics, OHSU School of Dentistry

Co-Authors: Ana Paula Piovezan Fugolin

Introduction:

The collagen degradation mediated by host proteolytic enzymes, such as the metalloproteinases (MMPs), is strongly associated to the development of secondary caries at the restorative material-dental tissues interface and periodontal disease. While some potent MMP inhibitors have been identified, their incorporation in the dental biomaterials remains as a challenge due to chemical incompatibility, poor diffusion, and limited substantivity. Therefore, this study is aimed at developing an innovative MMP-responsive nanocarrier to serve as a delivery vehicle for enzyme inhibitors and promote their sustainable and on-demand release.

Methods:

The newly designed nanocarrier is based on a micellar nanoparticle with the core composed of a block-copolymer and the shell of peptides with specific sequences of amino acids recognized and cleaved by the MMP-9. For the block-copolymer synthesis, the compounds (N-Benzyl)-5-norbornene-exo-2,3-dicarboximide (1) and 1-[[[(2S)-bicyclo[2.2.1]hept-5-en-2-ylcarbonyl]oxy]-2,5-pyrrolidinedione (2) were synthesized. The ring-opening metathesis polymerization was catalyzed by a modified Grubbs catalyst. The final block-copolymer was obtained via precipitation in cold methanol and centrifugation, and characterized by NMR spectroscopy.

The copolymer (50 mg/mL) was dissolved in an anhydrous mixture of dimethylformamide and dimethyl sulfoxide (DMSO) containing peptides with the amino acid sequence GPLGLAGGWGERDGS and N,N-Diisopropylethylamine (DIPEA) (1:4:16 copolymer:peptide:DIPEA). After stirring for 27 hr, the solution was precipitated in cold methanol and centrifuged—the peptide-copolymer was characterized by NMR spectroscopy.

To form micelles, the block copolymer-peptide compound was first dissolved in DMSO and distilled water was added via a syringe pump at 0.75mL/hr until reaching the critical micelle concentration (30% v/v aqueous). After 2 days of stirring, water was added via syringe pump at 5 mL/hr until reaching 50% v/v aqueous. The final solution was transferred to dialysis tubing and placed in water (pH=8). The buffer was exchanged 3x per day for 2 days, then the procedure was repeated once with Dulbecco's phosphate-buffered saline solution.

The micelles were characterized by transmission electron microscopy (TEM) after being concentrated. The responsivity to the MMP-9 was tested by incubating the micelles in a cleavage buffer for 24 hr at 37 °C, and further analyzed by TEM.

Results:

Stress, gel-point conversion and final conversion for all materials (Table 1) demonstrate that the addition of TMP reduced stress by 51%, while the introduction of DSDMA showed a modest increase in stress compared to controls. DABCO did not significantly affect stress. BisEMA+TMP exhibited the highest gel-point conversion (29.1±2.3%), while the gel-point conversion in the groups containing DSDMA was approximately half that of

the controls. The average final conversion at the completion of the gel-point conversion test was above 75% for all groups, with BisEMA+TMP showing the highest conversion ($96.4\pm 2.3\%$).

Conclusions:

The synthesized nanomicelles proved to be a promising delivery vehicle for encapsulation of MMP-inhibiting agents and other therapeutic drugs. The successful integration of peptides containing MMP recognition sequences is strong evidence for the potential of this platform to promote sustainable and on-demand drug delivery. In the next steps of this study, selected enzyme inhibitors will be sequestered into the micelles and their therapeutic efficiency at the adhesive interface and periodontal disease validated.

The color matching ability of single-shade composites

Kiyono (Kay) Koi (Yamashita)

Assistant Professor, Pfeifer lab, Department of Restorative Dentistry, OHSU School of Dentistry

Co-Authors: K. Koi, S. Amaya-Pajares, S. Kawashima, G. Arora, J.L. Ferracane, H. Watanabe,
Dept. of Restorative Dentistry, Oregon Health & Science University, Portland, Oregon;
H. Morisaki, Tokuyama Dental Corporation, Tsukuba-city, Ibaraki, JAPAN.

Introduction:

Manufacturers have been offering resin composites with various shade systems. The most popular system is a Vita-based multiple-shade system that requires shade selection at the chairside. These shade-matching tasks are challenging and time-consuming. In 2019, Tokuyama Dental launched the world's first One-Shade Universal Composite aiming to eliminate the shade-taking procedure by providing a composite that can blend with the surrounding tooth structure. Subsequently, other manufacturers developed their own one-shade universal composites. This study aimed to compare and evaluate the color matching of single-shade and traditional multiple-shade composites to extracted human natural teeth.

Methods:

Twenty extracted human teeth were polished with Optidisks and stored for 24 hours in water at 37 °C. An oval-shaped preparation (mesial-distal 2mm, incisal-gingival 5 mm, depth 2 mm) was created on facial or lingual surfaces of 10 extracted teeth from the light shade group (LSG) and 10 extracted teeth from the dark shade group (DSG). Preparations were restored with four single-shade composites—OMNICHROMA (OMC), Admira Fusion X-tra U shade (AFU), Essentia U shade (ESU), and Tetric EvoCeram T shade (TEC)—and two multiple-shade composites—Filtek Universal Restorative (FUR A1 and FUR A4)—and photopolymerized for 40 seconds using a curing light delivering 600 mW/cm² (Demi plus) followed by polishing with Optidiscs. After teeth were stored in water at 37 °C for 24 hours, color was measured using a spectrophotometer (CrystalEye). The ΔE^*00 value was calculated based on the color data of the unprepared tooth surface and the restoration. Composite placement and measurements were repeated three times per tooth. The analysis of variance (ANOVA) test was performed to compare the ΔE^*00 values between the groups ($\alpha=0.05$).

Results:

Among four single-shade composites, OMNICHROMA (2.49 ± 1.37) and Tetric (1.95 ± 0.79) showed the similar level of shade matching ability in light color natural teeth. The color matching ability of Tetric is greater than Admira (2.9 ± 1.55) and Essentia (3.26 ± 1.5) ($p<0.05$). Among four single-shade composites, OMNICHROMA (3.26 ± 1.31), Essentia (3.74 ± 1.83), and Tetric (3.31 ± 1.85) showed the similar level of shade matching ability in dark shade natural teeth. The ΔE^*00 value of Admira (5.17 ± 2.07) was significantly higher than other single-shade composites ($p<0.05$) in dark shade natural teeth. All single-shade universal composites showed better performance in shade matching in light shade than dark shade natural teeth. There was no statistical difference between the color difference values of OMNICHROMA and Filtek Universal Restorative (A1 and A4) in light and dark shade natural teeth. OMNICHROMA and Filtek Universal Restorative (A1 and A4) showed better performance in shade matching in light shade than dark shade natural teeth.

Conclusions:

OMNICHROMA showed the same level of shade-matching ability as Filtek Supreme in light- and dark-shaded teeth. Single-shade composites showed better color matching ability in the light-shaded teeth than dark-shaded teeth.

Stress and Gel-Point Conversion in Disulfide and Thiol-Modified Dental Resins

Steven Lewis

Research Project Manager, Pfeifer lab, Division of Biomaterials & Biomechanics, OHSU School of Dentistry

Co-Authors: Matthew Logan; Anissa Bartolome; Carmem Pfeifer

Introduction:

Stress reduction in dimethacrylates has been demonstrated with thiol additives, which effectively delay gelation/vitrification (Pfeifer, 2011). Additionally, -SH-containing materials may undergo esterification/disulfide bond exchange reactions in the presence of an amine near room temperature (Rekondo, 2014). This study investigated polymerization stress and network formation in resins containing a model disulfide to establish potential stress-reduction mechanisms in more complex thiol-based materials.

Methods:

BisEMA was mixed with 10mol% of Bis(2-methacryloyl)oxyethyl disulfide (DSDMA) or Trimethylolpropane tris(3-mercaptopropionate) (TMP), and 0 (controls) or 5mol% 1,4-Diazabicyclo[2.2.2]octane (DABCO), and 2,2-Dimethoxy-2-phenylacetophenone (0.2 wt%) as the initiator. Neat BisEMA was used as an additional control. Photocuring was conducted using a mercury arc lamp (Acticure, 320-500nm, 10 mW/cm²). Polymerization stress was assessed using the Bioman (10 min). Gel-point conversion, defined as the conversion at G'/G'' crossover, was measured using a coupled near-IR photorheometer (300µm thickness, 20mm diameter, 0.1% strain, 10Hz, 5 min, N₂ environment). Data (n=3) was analyzed with a one-way ANOVA/Tukey's test ($\alpha=0.05$).

Results:

Stress, gel-point conversion and final conversion for all materials (Table 1) demonstrate that the addition of TMP reduced stress by 51%, while the introduction of DSDMA showed a modest increase in stress compared to controls. DABCO did not significantly affect stress. BisEMA+TMP exhibited the highest gel-point conversion (29.1±2.3%), while the gel-point conversion in the groups containing DSDMA was approximately half that of the controls. The average final conversion at the completion of the gel-point conversion test was above 75% for all groups, with BisEMA+TMP showing the highest conversion (96.4±2.3%).

Conclusions:

The results suggest TMP effectively delays gelation and reduces polymerization stress due to chain-transfer events. However, the addition of amine does not appear to affect polymer network properties of DSDMA-modified materials. Future experiments with dynamic mechanical analysis will be used to decouple potential disulfide exchange from other mechanisms in more complex thiol-based materials.

Exploring GtfC Inhibition via a Fluorescent Sugar Assay

Matthew Logan

Instructor, Division of Biomaterials & Biomechanics, OHSU School of Dentistry

Co-Authors: Matthew Logan, Marcelo Icimoto, Alexander Kendall, Sarah Patty, Carmem Pfeifer

Introduction:

The development of biofilms on dental restorations may lead to the formation of secondary caries. Previously, a small library of potential inhibitors (G43 family – Wu 2017) was synthesized and screened for inhibition/disruption of *S. mutans* biofilms using crystal violet staining and polysaccharide connectivity assay. These compounds were further studied with an assay utilizing a fluorometric sugar to yield kinetic parameters and give greater insight into the inhibitory nature of this family of compounds.

Methods:

The inhibitor compounds were dissolved in DMSO and serially diluted in PBS to 50 μ M and 5%vol DMSO. After 30 minutes incubation with the GtfC purified enzyme at room temperature, the fluorescent sugar substrate, 4-Nitrophenyl- β -D-glucopyranoside (pNPG), was added and the absorbance at 400 nm was recorded. The inhibitors were compared to a DMSO control to determine the percent of GtfC activity. Data were analyzed with one-way ANOVA/Tukey's test ($\alpha=5\%$). The most promising compound from this work and previous studies, G43-C3-TEG, was repeated at varying concentrations of sugar substrate to construct a Michaelis–Menten plot.

Results:

At 50 μ M, all G43 derivatives showed similar amounts of GtfC inhibition although not particularly potent (46-55% GtfC activity), $p = 0.05$. Based on the direction G43 enters the active site, some methylated derivatives should perform better than others. The lack of significant differences among derivatives indicates a lack of specificity. In previous studies, G43-C3-TEG has performed the best, showing obvious biofilm disruption; however, in this study, it performed similarly to other derivatives.

Conclusions:

Although the G43 family of derivatives has shown promise in disrupting biofilm, due to lack of potency and specificity, it appears that the disruption is not solely attributable to Gtf enzyme inhibition. Future work will include further exploration into mechanisms that could be responsible for the observed biofilm disruption as well as pursuing a more potent inhibitor.

CHX or DOX-loaded TiO₂-nanotubes adhesives as anti-MMP strategy

Fernanda Lucena

PostDoctoral Fellow / R90 PORT Trainee*, Pfeifer lab, Division of Biomaterials and Biomechanics,
OHSU School of Dentistry

Mentor: Carmem Pfeifer

Co-Authors: Erika Soares Bronze-Uhle, Marjorie de Oliveira Gallinari, Diana Gabriela Soares dos Passos, Adilson Yoshio Furuse (Department of Endodontics, Operative Dentistry and Dental Materials, Bauru School of Dentistry, University of São Paulo);

Paulo Noronha Lisboa-Filho (São Paulo State University - Unesp, School of Sciences, Department of Physics);

Carla Castiglia Gonzaga (Department of Dentistry, Universidade Positivo);

Matthew Logan, Carmem Pfeifer (Division of Biomaterials and Biomechanics, OHSU)

Introduction:

This study aimed to characterize a dental adhesive modified by the incorporation of dioxide titanium nanotubes (TiO₂-nts), functionalized with 3-aminopropyl trimethoxysilane (APTMS), loaded with chlorhexidine (CHX) or doxycycline (DOX) to be used as MMP inhibitors and potentially increase the longevity of the bonded interface of composite restorations.

Methods:

TiO₂-nts were produced by alkaline synthesis and loaded with CHX or DOX at 0 (control) or 10w/v or 30w/v%, respectively. All TiO₂-nts were characterized by X-ray diffraction (XRD), scanning electron microscopy (SEM), energy-dispersive X-ray spectroscopy (EDS), thermogravimetric analysis (TGA), and transmission electron microscopy (TEM). Then, the nts were added at 5w/v% to Single Bond Universal (3M-ESPE) adhesive for evaluation of inhibition of total MMP activity, degree of conversion (DC), microtensile bond strength (μ TBS), and transdental cytotoxicity in human dental pulp cells (HDPCs). Data were analyzed with ANOVA/Tukey's test and Student's t-test with a 5% significance level.

Results:

XRD patterns confirmed the anatase phase of TiO₂-nts, SEM and TEM images demonstrated the tubular and hollow morphology of TiO₂-nts, with average diameter of 19.6 (3.0) nm, and length of 162 (48) nm. The EDS and TG analyses showed an efficient APTMS-functionalization and encapsulation of the inhibitors (CHX and DOX). All modified adhesives containing CHX or DOX were able to reduce total MMP activity between 65-72%. Adhesives modified by APTMS-functionalized TiO₂-nts groups presented higher DC when compared to the non-functionalized. For both etch-and-rinse (ER) and self-etch (SE) modes of application, CHX and DOX-loaded TiO₂-nts were able to sustain μ TBS after 6 months storage in saliva. All modified adhesives presented higher cell viability when compared to the SBU control.

Conclusions:

Given the results obtained in this study, the functionalized and non-functionalized TiO₂-nts were successfully incorporated into a BisGMA/HEMA-based commercially available adhesive, showing a potential application for MMP inhibition and bond preservation.

**PORT (Portland Oral Health Research Training) T90/R90 Program is an OHSU School of Dentistry training program, funded by NIH/NIDCR, that supports mentored training in oral and craniofacial health research to PreDoctoral, Dual Degree, PostDoctoral, and Foreign-Trained Dentist trainees.*

Design and validation of a co-polymerizable MMP inhibitor

Luke Miller

Senior Research Associate, Pfeifer lab, Division of Biomaterials & Biomechanics, OHSU School of Dentistry

Co-Authors: Luke Miller, Matthew Logan, Fernanda Sandes De Lucena, Marcelo Icimoto, and C. S. Pfeifer

Introduction:

Matrix metalloproteinases (MMPs) have been shown to decrease the stability of the bonded interface through collagenolytic activity. A well-studied and potent hydroxamic acid MMP inhibitor, NNGH, was chosen as a scaffold for the design of a co-polymerizable restorative material capable of long-lasting inhibition of MMPs. This study works to design and validate hydroxamic acid derivatives to characterize the area protein leading out of the active site and to identify a candidate compound for functionalization with a linker and polymerizable moiety.

Methods:

Hydroxamic acid derivatives of the parent inhibitor compound, NNGH, were designed and synthesized with terminal methoxy groups and linkers of varying length and polarity. A carboxylic acid version of NNGH was used to represent the hydrolysis of the zinc binding hydroxamic acid. Derivatives were modeled (Chimera/Autodock) in active site of MMP2/9 and given a docking score. MMP activity was determined using a commercial kit (EnzChek Gelatinase/Collagenase Assay Kit; Molecular Probes). Data were fit to a non-linear curve (one phase decay) to determine IC50 values.

Results:

The parent molecule, NNGH, had the best docking score, -6.5 kcal/mol, and most potent IC50, $0.16 \pm 0.06 \mu\text{M}$. The trend observed in docking scores was also observed in IC50 values, with NNGH performing the best, and the carboxylic acid analog, NNGC, performing the worst (368x reduction). Hydroxamic acids bind much tighter to zinc than carboxylic acids so this trend is expected. The linker derivative, NNGH-2, did have reduced potency (28x reduction), the fact that it was much less reduction than NNGC is evidence that linker (terminal methoxy) did not disrupt the compounds fit into the active site enough to disrupt zinc binding.

Conclusions:

Although less potent, NNGH-2 provides evidence that the NNGH scaffold has potential to be functionalized as a co-polymerizable restorative material. Further derivative synthesis and analysis is needed to optimize the compound for a linker.

Thiol Content Determination of Thiourethane Functionalized Fillers for Dental Composites

Clara Park

DMD Student, Pfeifer lab, Division of Biomaterials & Biomechanics, OHSU School of Dentistry

Mentor: Carmem Pfeifer

Co-Authors: SS Patty, MG Logan, SH Lewis, SF Weber, CS Pfeifer

Introduction:

The purpose of this study was to develop a method for characterizing thiol content [SH] on inorganic fillers functionalized with thiourethane oligomers (TU), capable of consistently capturing [SH] over several orders of magnitude concentration.

Methods:

TU and TU-functionalized fillers were produced as previously described (Faria-e-Silva, 2018). [SH] was determined by a modified iodometric titration method. In brief, I₂ was added in excess to reduce the -SH, in a solution containing KI/glacial acetic acid (aq). After initial bleaching, residual I₂ was titrated with Na₂S₂O₃(aq) in the presence of a starch indicator, until color disappeared. The [SH] was calculated based on the reducing titrant required to consume the excess I₂. Varied amounts of the starting TU and the corresponding functionalized fillers (BaBSO₄ glass, 0.7 μm) were titrated. Unfunctionalized fillers were titrated to establish a baseline correction. Thermogravimetric analysis was used to determine TU content on the filler surface and estimate the expected [SH]. Correlation plots were built for the calibration curves.

Results:

Figure 1a/b show the calibration curves (mass added vs. titrating required) of the corresponding TU oligomer/filler pair. As expected, the titrant concentration needed for the filler is two orders of magnitude lower. This is due to the expected lower [SH] on the filler, and to increased time-scale of SH-I₂ interactions when the TU is tethered to the surface. Figure 1c demonstrates that the measured [SH] linearly correlated with the calculated [SH].

Conclusions:

This modified iodometric titration method demonstrates a robust, repeatable approach for characterizing thiol content of novel TU oligomers and their subsequent oligomer-functionalized particles. The molality of functionalized filler was consistently 50-60% of the theoretical functionalization predicted by TGA weight loss, suggesting oxidation independent of what species was tethered to the filler surface. This method is more repeatable to determine [SH] on surfaces compared to standard Ellman's titrations.

Carboxybetaine-based switching molecule to attack/defend against bacteria

Sarah Patty

Research Associate, Pfeifer lab, Division of Biomaterials & Biomechanics, OHSU School of Dentistry

Co-Authors: M. Logan, G. Guimaraes, M. Icimoto, L. Borges, S. Lewis, A. Furuse (Operative Dentistry, Endodontics and Dental Materials, Bauru School of Dentistry, Bauru, SP, BRAZIL), C.S. Pfeifer

Introduction:

Biofilm colonization on biomedically-relevant surfaces is one leading cause of reinfection in dental restorations. The existing antifouling and/or antimicrobial materials are efficient in either preventing attachment or killing bacteria, but much more effective protection could be achieved if both properties were combined. Thus, our goal was to take advantage of natural pH variations in the oral cavity to design a reversible molecule (carboxy betaine – CB-000), alternately existing in two chemical states: an antibacterial quaternary ammonium cation (through acid-catalyzed ring closure), and an antifouling linear zwitterion. Methyl-substituted derivatives have been synthesized to tailor the switching equilibrium closer to physiological pH (CB-200).

Methods:

The viability of *Streptococcus mutans* bacteria was evaluated by bioluminescence (Luciferase Assay) and Crystal Violet (CV). The switching compounds CB-000 (pH=1), CB-200 (pH=3), a non-switching antibacterial control (CTAC) and a non-switching zwitterion control (MPC) were tested at a range of pH values (3.0-7.0), added at 50 μ M to the culture medium for mature biofilm grown at pH 7, or prior to bacteria inoculation at each pH. Data were analyzed by two-way ANOVA/Tukey's test ($\alpha=5\%$).

Results:

The figure show results for luciferase metabolic assay and biomass. Both assays demonstrate that the biofilm growth at pH 3-4, as expected, was slow/low, which led to no appreciable difference among the groups ($p<0.05$). At pH 5-7, only CTAC affected bacterial metabolism/growth, indicating that both CB molecules were in their linear/zwitterionic state, as expected, and had no bactericidal effect. In addition, the CB molecules used here had a one-carbon side chain, which does not allow for charge concentration (pseudo-micellization), in turn needed to be effective against gram+ bacteria.

Conclusions:

This study confirmed that the CB derivatives tested here are stable as zwitterions at higher pH. Future studies will utilize longer side chains/higher degree of substitution for charge concentration/switching at higher pH.

Influence of synthesis parameters on the structure and stability of poly(urea-formaldehyde) microcapsules

Sivashankari Rajasekaran

PostDoctoral Fellow, Fugolin lab, Department of Restorative Dentistry, OHSU School of Dentistry

Mentor: Ana Paula P. Fugolin

Co-Authors: Bao Huynh and Ana Paula P. Fugolin

Introduction:

Microencapsulation is an advanced technology that ensures stability and on-target delivery of therapeutic compounds. Poly(urea-formaldehyde) (PUF) microcapsules have been used for several years for various applications ranging from encapsulation of oils to paints. There are several methods and parameters to obtain PUF microcapsules however, shell stability and preservation of the encapsulated volume of therapeutic compounds remain as challenges. In the present work, we have investigated the effect of synthesis parameters such as core/shell ratio, micro-emulsification method, and therapeutic agent properties on the structure and stability of microcapsules designed for self-healing dental polymers.

Methods:

Double micro-emulsification technique was used to encapsulate a hydrophobic (100 wt% TEGDMA - triethylene glycol dimethacrylate) and a more hydrophilic (80 wt% TEGDMA + 20 wt% DMAM - N, N-Dimethylacrylamide) healing agents in PUF shells at core/shell ratios of 3/1, 4.5/1, 6/1, 7.5/1 and 9/1. In this technique, the healing agent system (oil phase) is encapsulated via oil-in-water double emulsion stabilized by ethylene-maleic anhydride (surfactant) in an ammonium chloride-catalyzed reaction between urea, resorcinol, and formaldehyde (water phase). Fluorescence labelling of the healing agents with DCM (4-(Dicyanomethylene)-2-methyl-6-(4-dimethylaminostyryl)-4H-pyran) at 1.5 wt% was used to enable clear distinction between shell and core components. For microemulsion formation, three different methods were tested: magnetic stirring (400 rpm), ultrasonic homogenization (40% intensity), and mechanical/overhead stirring (400 rpm). After synthesis, the microcapsules were rinsed with hexanes, vacuum filtered, and dried for 24 h at room temperature. Morphologic characterization of the newly synthesized PUF microcapsules was performed by optical microscopy. Polydispersity and average diameter of the microcapsules were assessed by processing the optical micrographs using the ImageJ software. The actual reaction yield of each reaction (%) was calculated and the encapsulation efficiency (%) was obtained by extraction in acetone method.

Results:

Formation of microcapsules was observed in all experiments irrespective of the difference in synthesis parameters. Changes in the core/shell ratio parameter impacted dramatically the reaction yield, the microcapsules size, and shell stability. The ratio 6:1 resulted in the most efficient chemical reaction with percentage yields 30% higher than the other groups. Other core/shell ratios resulted in larger concentration of broken microcapsules with very low yield (from 9% to 20%). Therefore, 6:1 was fixed as the core/shell ratio and different micro-emulsification methods were tested. The reaction yield of microcapsules using magnetic stirring, ultrasonic homogenization and mechanical stirring were 45%, 41% and 67%, respectively. The diameter ranged from 20 to 300 μm for the microcapsules prepared using magnetic and mechanical stirring, whereas ultrasonic homogenization resulted in microcapsules of 5 to 20 μm in diameter. In relation to the healing agent's systems, there are not any significant differences between the groups, which highlights that

the optimizations carried on the PUF systems made the shells sufficiently robust to sequester both hydrophobic and hydrophilic compounds and maintain them confined in their core.

Conclusions:

In the present work we have successfully prepared poly(urea-formaldehyde) microcapsules by varying the core/shell ratio, micro-emulsification method and composition of healing agents. The results show that microcapsules obtained using 6:1 core/shell ratio were optimal for further studies. Changing the micro-emulsification method resulted in microcapsules of varying sizes, which seems to be a promising strategy to tailor the carriers according to the therapeutic niche requirements. Finally, the optimized PUF system proved to be capable of encapsulating agents with distinct degrees of hydrophobicity, which may broaden the technique application.

Does salivary pellicle affect the antibacterial efficacy of QAM-based composite?

Noor Saeed

DMD Student, Pfeifer lab, Division of Biomaterials and Biomechanics, OHSU School of Dentistry

Mentor: Genine Guimarães

Co-Authors: L.P. Borges, L. Correr-Sobrinho, Restorative Dentistry, Dental Materials division, University of Campinas, Piracicaba, Sao Paulo, BRAZIL;

N. Saeed, L.P. Borges, M. Logan, S. Lewis, M. Icimoto, C.S. Pfeifer, School of Dentistry, Oregon Health & Science University, Portland, Oregon, UNITED STATES.

Introduction:

The efficacy of any antibacterial coating depends on their ability to directly contact the microorganisms they seek to eliminate. In the oral cavity, all surfaces are almost immediately coated with a layer of proteins known as the acquired salivary pellicle (ASP) once in contact with saliva. In this study, the antibacterial efficacy of a quaternary ammonium methacrylate (QAM) was tested in the presence of ASP, in terms of surface charge density and overall *S. mutans* elimination.

Methods:

One commercial composite (Filtek Supreme, 3M-ESPE) and experimental methacrylate composites with 0 (control) or 10wt% quaternary ammonium methacrylate (QAM-C16), containing photoinitiators and 70wt% of inorganic fillers were used to fabricate discs (10 mm diameter and 1.5 mm thickness, n=6), light-cured for 40 s. Saliva was obtained from donors who abstained from brushing teeth for 24 hours or have food/drink intake 2 hours prior to collection. Saliva was processed cold, and sterilized, and used to produce ASP on disc surface (1mL, 2 hours). Discs were then transferred to 24-well plates containing aliquots (1mL) of bacterium TH medium (10 μ L Bioluminescent *S. mutans*) at a 5% CO incubator for 24 hours. Bioluminescence activity and surface charge density were measured in a microplate reader (SuperMax D3). Data was analyzed with two-way ANOVA/Tukey's test ($\alpha=5\%$).

Results:

Results indicated significant reduction on the biofilm growth for QAM composite regardless of the presence of an ASP compared to the control groups (Figure 1A). Higher surface charge density ($p<0.0001$) was observed for QAM composites compared to other groups (Figure 1B). Presence of an ASP reduced the surface charge density for QAM ($p<0.005$).

Conclusions:

The presence of acquired salivary pellicle did not interfere with the antibacterial efficacy of a quaternary ammonium monomer, in spite of the reduction in surface charge.

Dental Student Provision of Tobacco Cessation Advice and Assistance

Chris Steiner

DMD Student, OHSU School of Dentistry

Mentor: Dr. Sue Flocke

Co-Authors: Sue Flocke

Introduction:

Tobacco use adversely impacts oral health, thus, addressing tobacco use is important in the dental setting. The dental tobacco cessation counseling (TCC) training was developed as part of routine curriculum at OHSU. Performing the tobacco assistance was supported by a form in the EHR and this was also used to track performance of tobacco assessment and assistance. This study is designed to evaluate the degree to which students do the recommended tobacco assistance protocol and to examine performance by visit type and year in dental school.

Methods:

A retrospective chart review was completed consisting of data from 420 student providers and 12,623 visits from 7/1/2017 to 6/30/2022. The tobacco assistance protocol was based on the 5A of tobacco cessation assistance--Ask about tobacco status, Advise to quit, Assess readiness to quit, Assist to quit with referral to counseling and provision of FDA approved cessation medications and Arrange follow-up. Descriptive statistics of performance of the tobacco assistance protocol (each A and overall appropriateness of tobacco assistance) are reported. Appropriateness was defined in the follow way: Ask, Advise and Assess readiness is expected of all visits; Assistance (offer of counseling and/or medications and setting a quit date) and Arrange follow-up should be offered for patient who report being ready to quit. The association of tobacco assistance by 3rd vs. 4th years and by visit type (preventive focused or comprehensive vs. procedure focused) was examined using Chi Square tests.

Results:

During the study time period, there were 12,623 patient visits. The TTC form was completed for 502 visits, and the patient reported using some form of tobacco in 458 instances. Advise was completed in 97% of visits; assess readiness in 87% of visits. Of the 28% patients that indicated they were 'Ready Now' to quit, assistance was provided 92.1% of the time, and a quit date was set 61.1% of the time. 3rd year students were significantly more likely to use the TCC form than 4th year counterparts (4.1% vs 2.2% respectively, $P < 0.01$). Comparing comprehensive visits to procedural visits, use of TTC was not significantly different (3.0% vs 3.4%, $P = 0.20$).

Conclusions:

Overall uptake of the tobacco protocol was poor. However, when used by a student, completion of protocol steps was good. Proximity to training and comprehensive visits were associated with higher rates of completion, but the effect was small. Proximity to training may influence the frequency and completeness of TCC and explains why the 3rd year students demonstrate a higher performance. Efforts to improve student uptake are needed to better understand if the tobacco cessation training received by students has been adequate.

Mechanical properties, bond strength and surface characterization of 3Y-TZP after different surface treatments protocols

Fernanda Tsuzuki

Visiting PhD Student, Pfeifer lab, Division of Biomaterials & Biomechanics, OHSU School of Dentistry

Mentor: Carmem Pfeifer

Co-Authors: Fernanda Midori Tsuzuki, Evaldo Pinheiro Beserra Neto, Monique de Souza, Mauro Luciano Baesso, Américo Bortolazzo Correr, Ana Rosa Costa, Lourenço Correr Sobrinho, Carmem Pfeifer

Department of Restorative Dentistry, Dental Materials Division, Piracicaba Dental School, UNICAMP, State University of Campina, Piracicaba, SP, Brazil

Physics department, State University of Maringa, Maringá, PR, Brazil

Oregon Health & Science University, School of Dentistry, Biomaterials and Biomechanics, Portland, OR, USA

Introduction:

Due to its rigid and crystalline nature, yttria-stabilized zirconia (3Y-TZP) the adhesion to the cement material is challenging. Currently, the most used surface treatment protocol for 3Y-TZP is sandblasting with alumina particles, which makes zirconia more susceptible to cracking, fracture and long-term degradation. Therefore, the aim of this study was to evaluate the mechanical properties and the microshear bond strength (μ SBS) of zirconia after sandblasting with 50 μ m Al₂O₃ particles at different sintering stages with varying pressure.

Methods:

Al₂O₃ sandblasting (50 μ m) on IPS e.max Zircad zirconia samples was performed as follows: (1) before sintering (PRE), (2) before and after sintering (PRE/POS) and (3) after sintering (POS), with pressure variation of 2, 3 and 4 bar. A group without treatment was used as a control (n=22). Phase transformation analysis was performed through Raman spectroscopy. Confocal Laser Microscopy was used to analyze the zirconia surface roughness (Sa) and to produce 3D topographic images. Therefore, three cylinders of Panavia V5 resin cement were adhered to the ceramic, stored for 24 hours at 37°C and submitted to Microshear bond strength (μ SBS) (1mm/min). Zirconia samples were subjected to the three-point flexure resistance test (FR) in a universal testing machine (Load was applied in the center with a loading rate of 1.0mm/min and a load cell of 5000 kgf). For Scanning Electron Microscope (SEM) analysis, two random specimens from each group were evaluated. Data were tested for normality (Shapiro-Wilk) and homoscedasticity (Levene's Test). μ SBS and FS were subjected to two-way ANOVA (type of treatment and pressure variation) and Tukey's post hoc test. Sa and SFE were analyzed by a non-parametric analysis using the Kruskal-Wallis and Dunn's tests. The level of significance was set for all tests at 95% ($\alpha=0.05$). The roughness images and micrographs were evaluated using descriptive analysis.

Results:

The groups that were blasted with a pressure of 4 bar had the highest Sa values ($p<0.05$). 3D images of untreated samples revealed a homogeneous surface. Samples treated with higher pressures showed more heterogeneous surfaces. The Raman peaks related to the presence of the monoclinic phase were observed in the PRE/POS and POS groups. PRE/POS ($p<0.001$) and POS ($p=0.005$) showed higher μ SBS values than the PRE group. The lowest μ SBS values were presented by Control (2.5 MPa). Most failures were adhesive in Control and all PRE groups. In the other groups, when sandblasting was performed, an increase in mixed and cohesive

failure could be observed. The lowest FS value was presented by Control (691.13 MPa) which was significantly different from PRE/POS4 (986.72 MPa), POS2 (965.60 MPa), POS3 (1075.20 MPa) and POS4 (992.86 MPa) groups.

Conclusions:

It can be concluded that higher pressures increased the surface roughness of zirconia. In addition, regardless of the pressure, the sandblasting performed before/after, and only after sintering showed higher microshear bond and higher flexural strength values. Therefore, sandblasting can be done before and after, or just after, but never just before sintering using pressures of 3 and 4 bar.

Bond Strength and Polymerization Kinetics Study of Acrylamide Adhesive Formulations

Samuel Weber

Senior Research Assistant, Pfeifer lab, Dept of Biomaterials and Biomedical Sciences, OHSU School of Dentistry

Co-Authors: Steven H. Lewis and Carmem S. Pfeifer

Introduction:

The co-polymerizations of acrylamides/methacrylates can be complicated by differential reactivities and interpenetrating network formation. The bond strength and conversion of experimental dental adhesives containing methacrylate/acrylamide pairs were investigated as a function of the addition of an iodonium salt co-initiator.

Methods:

BisGMA or UDMA were mixed with a tertiary tri-acrylamide (TMAAEA) or 2-hydroxyethyl methacrylate (HEMA) in a 60:40 wt% ratio, and CQ/EDMAB/BHT (0.2/0.8/0.5 wt%) as the initiator system. Diphenyliodonium hexafluorophosphate (DPI-PF6) was added at 0 (control) or 0.4 wt%. Polymerization kinetics was assessed in near-IR during photoactivation with 1000 mW/cm² for 20 s (470 nm, Elipar, 3M-ESPE). Solvated materials (40 vol% ethanol) were used to bond two 2 mm layers of composite (Filtek Supreme Ultra, 3M-ESPE) onto exposed coronal dentin of caries-free human third molars (Elipar). Microtensile bond strength (MTBS, in MPa) samples (1 mm² sticks) were stored in milliQ water or culture medium containing *S. mutans* for one week, before being tested at 0.5 mm/min. Data were analyzed with three-way ANOVA/Tukey's test (alpha=5%).

Results:

All three factors (base, diluent and presence of DPI-Pf6) affected MTBS in water, biofilm, conversion and RPmax ($p=0.000$ for all factors and most interactions). When DPI-Pf6 was added, the triacrylamide adhesives presented greater MTBS in water and biofilm compared with HEMA monomers for both BisGMA and UDMA-based materials. The addition of DPI-PF6 increased MTBS HEMA and TMAAEA adhesives in both base monomer systems. In general, the HEMA-containing adhesives showed higher conversion and RPmax within the same base/DPI-Pf6 condition. Therefore, no correlation was found between conversion and MTBS in this study, which can be explained by the fact that the kinetics was measured in the unsolvated adhesives.

Conclusions:

This study demonstrates that using a crosslinking monomer in the adhesive formulation improves the stability of the bond under clinically-relevant solvated conditions. However, the acrylamide required an iodonium salt for optimal performance.

Filler Size Effects Surface Properties of Composites Pre-/Post-Toothbrush Abrasion

Sarah Wiskoski

DMD Student, Ferracane lab, Dept of Oral Rehabilitation and Biosciences, OHSU School of Dentistry

Mentor: Jack Ferracane

Co-Authors: Kobayashi, Mikihiro (visiting Professor, Showa University, Tokyo, Japan); Koi, Kiyono; Lewis, Steven; Ferracane, Jack

Introduction:

Surface gloss and roughness significantly affect the esthetic properties of dental composite restorative materials. This study aimed to investigate the effect of different-sized spherical fillers on the surface gloss and surface roughness of polished resin composites before and after toothbrush abrasion.

Methods:

Five experimental light-cure resin composites were formulated with a light-curable resin of equal mixture Bis-GMA/UDMA/TEGDMA and different-sized spherical zirconia-silica fillers (RC60 = 60 nm size at 50 wt%; and RC-150 = 150 nm size; RC-270 = 270 nm size; RC-400 = 400 nm size; RC-700 = 700 nm size, these all with 70 wt% filler) treated with γ -MPTS, and compared with OMNICHROMA, a commercial composite with 79wt% of similar filler of 260 nm size. Thirty rectangular specimens (Width=12mm, Depth=5mm, Height=2mm) were made by light-curing for 40 seconds (600 mW/cm², Demi Plus) through a mylar matrix from the top and bottom. All specimens (n=5) were hand polished with a standardized sequence with #1200, #2400, and #4000 SiC papers (each 60s). Before and after tooth brushing in a custom device for 60, 180, and 360 min (1 Hz; Crest Pro-Health), five gloss (GU) measurements were made on each specimen using a Novo-curve gloss meter (60°). The surface roughness (Ra) of the specimens before and after toothbrushing were measured using a surface profilometer (TR200; cut-off length 0.8 mm, measuring length 2 mm) in three different regions. Data were analyzed with one-way ANOVA/Tukey's test (alpha=0.05). Pearson's correlation coefficients between the gloss and surface roughness and filler size were also calculated.

Results:

Surface gloss decreased, and the surface roughness increased after brushing for all materials. RC-60 showed significantly higher GU values, and RC-700 showed significantly lower GU values after the toothbrush test. A significant correlation was found between GU and Ra and filler size before and after toothbrushing.

Conclusions:

Filler particle size influenced the GU and Ra of the experimental composites after toothbrush abrasion, with the materials with the smallest spherical fillers maintaining gloss and smoothness better than those with the larger spherical fillers. Gloss decreased due to the increase in surface roughness of resin composite after the toothbrush abrasion. While many factors may affect the surface properties of dental composites before and after being exposed to toothbrush abrasion, this study emphasizes the importance of filler particle size due to the fact that the composition, shape and concentration of fillers was the same, and only size differed among the experimental composites.

A bone metastasis on-a-chip approach to study the preferential growth of cancer cells into bone

Avathamsa Athirasala

PostDoctoral Fellow and PORT T90 Trainee*, Bertassoni lab,
Dept of Oral Rehabilitation & Integrative Biosciences, OHSU School of Dentistry

Mentor: Luiz Bertassoni

Co-Authors: Amin Mansoorifar, Cristiane Miranda Franca, Maria Elisa Lima Verde, Ramesh Subbiah, Ryan Gordon, Luiz E Bertassoni

Introduction:

Several neoplastic diseases have bone as the preferential site for metastasis, which usually has a substantially different microenvironment when compared to the primary tumours. However, current in-vitro bone models fail to replicate the structural and cellular complexity of bone tissue. The intrafibrillar collagen mineralization, presence of osteoblasts, osteocytes, and pericyte-supported vasculature are some of the key hallmarks of bone microenvironment. Additionally, the effect of the collagen nanoscale mineralization of bone matrix as promoter of cancer metastasis remains unknown, despite existing evidence suggesting that this may be a decisive factor in increasing cancer aggressiveness.

Methods:

In this study, engineered and validated a novel bone-on-a-chip platform that mimics the microenvironmental and biological features of native bone. Thereafter, we used this device to demonstrate and track the process of extravasation of tumor cells through the pericyte-supported vasculature and into a cell-laden nanoscale calcified matrix in real-time and the resultant changes to tumor cell phenotype.

Results:

Our results suggest that the presence of nanoscale intrafibrillar collagen mineralization promotes a change in cancer cell phenotype, resulting in significantly more invasion of tumor cells into the bone matrix than non-calcified collagen.

Conclusions:

This platform provides a unique model to elucidate key mechanisms of cancer metastasis into bone.

**PORT (Portland Oral Health Research Training) T90/R90 Program is an OHSU School of Dentistry training program, funded by NIH/NIDCR, that supports mentored training in oral and craniofacial health research to PreDoctoral, Dual Degree, PostDoctoral, and Foreign-Trained Dentist trainees.*

RegendoGEL: A novel tooth-derived hydrogel for pulp & dentin regeneration

Anissa Bartolome

Senior Research Assistant, Dept of Oral Rehabilitation & Integrative Biosciences, OHSU School of Dentistry

Co-Authors: Anissa Bartolome-1, 4, Cristiane Miranda Franca-1, 4, Weibo Zhang-5, Scott Olson-6, Pamela Yelick-5, 6, Luiz Bertassoni-1, 2, 3, 4, 6

1. Division of Biomaterials and Biomechanics, Department of Restorative Dentistry, OHSU School of Dentistry
2. Center for Regenerative Medicine, OHSU School of Medicine
3. Department of Biomedical Engineering, OHSU School of Medicine
4. Cancer Early Detection Advanced Research (CEDAR), Knight Cancer Institute
5. Department of Orthodontics at Tufts University School of Dental Medicine
6. RegendoDent Inc.

Introduction:

Dental caries are a major health concern often requiring endodontic treatment, of which 15M are performed annually in the US. Current endodontic treatments essentially kill the tooth by removing the dental pulp and replacing it with a non-degradable, cement-like material. OHSU, Tufts University, and their collaborative spin-out company, RegendoDent, Inc., has developed a novel clinical product intended for vital pulp therapies. The product, RegendoGEL, contains key stimulatory molecules found in healthy teeth that naturally promote dental pulp repair and regeneration. This study tests inflammatory infiltrate in the dental pulp and dentin formation in tooth samples treated with RegendoGEL versus a silicate cement.

Methods:

In this study, an in vivo animal model was used to perform a pulpotomy consisting of four experimental groups: RegendoGEL, gelatin methacryloyl (GelMA), collagen, and mineral trioxide aggregate (MTA). Teeth from experimental animals were evaluated on days 5 and 70 for inflammation and tertiary dentin formation. MicroCT and histological analyses were conducted for both timepoints. Inflammatory scores were based on the ISO recommendation, which 0 is for no inflammation, 1 for mild, 2 for moderate, and 3 is for the presence of severe inflammatory infiltrate.

Results:

The study revealed that RegendoGEL elicits little to no inflammatory response (0-1) while promoting tertiary dentin formation. Quantitative analysis of tertiary dentin formation was observed in all roots from teeth filled with RegendoGEL, followed by GelMA, MTA, and collagen. After 5 days, RegendoGEL induced thicker mineral deposition and tertiary dentin formation as compared to MTA. After 70 days, RegendoGEL and MTA presented thicker deposits of tertiary dentin as compared to collagen.

Conclusions:

These data suggest that RegendoGEL may be used as a better alternative to conventional silicate cements. Further studies are currently being planned to determine the best form factor of this material. Clinician feedback on product handling will also be valuable information to have before product launch.

Perivascular cells mediate collagen stiffness and architecture sensing in blood vessels

Cristiane Franca

Research Assistant Professor, Dept of Oral Rehabilitation & Integrative Biosciences, OHSU School of Dentistry

Mentor: Luiz Bertassoni

Co-Authors: Maria Elisa Quezado Lima Verde, Amin Mansoorifar, Avathamsa Athirasala, Ramesh Subbiah, Anthony Tahayeri, Rahul M. Visalakshan, Luiz E. Bertassoni

Introduction:

Microvasculature homeostasis is established through a dynamic interaction of endothelial cells (EC), perivascular cells (PC) and the extracellular matrix (ECM). Type I collagen is the most abundant ECM component. Also, collagen changes in stiffness, density and crosslinking can be seen in conditions associated with abnormal angiogenesis, such as fibrosis and cancer. Both EC and PC are mechanosensitive, changing their phenotype and function in stiffer environments. However, the precise role of PC in sensing the ECM's mechanical status is still unclear.

Methods:

To address this knowledge gap, we used an organ-on-a-chip device to engineer PC-supported blood vessels. Briefly, 160- μ m channels were engineered using type I collagen that underwent fibrillogenesis at different temperatures (4, 16, 21 and 37°C). Thus, the microarchitecture and stiffness would vary from a soft reticular network (37°C) to a stiff fibrillar mesh (4°C). We then seeded human umbilical vein endothelial cells (HUVECs) and mesenchymal stem cells (MSCs) in the collagen channels. After 48h, samples were fixed and stained for actin (cytoskeleton), NG2 (pericyte differentiation), and CD31 (endothelial cell junction), imaged with a confocal microscope and analyzed with Imaris. A gene analysis with Nanostring was performed.

Results:

Microvessels engineered in contact with a softer reticular collagen showed more pericyte differentiation ($p < 0.05$), inter-endothelial cell junctions ($p < 0.05$), and effective barrier function. In contrast, stiffer fibrillar collagen was associated with cell migration outward the vessel, leakiness, and higher RNA expression of transforming growth factor beta, vimentin, and collagen III. When vessels were engineered without pericytes, those differences were drastically minimized.

Conclusions:

In conclusion, perivascular cells may have a major effect in sensing the differences in collagen architecture and guiding vessel integrity. Moreover, collagen architecture and stiffness affect PC differentiation, vascular morphology, and function.

Single Cell Bioprinted Cell Circuits for the Systematic Assessment of Cell-Cell Communication in the Early Tumor Microenvironment

Haylie Helms

PhD Student and former PORT T90 Trainee*, Bertassoni lab,
Department of Oral Rehabilitation and Integrative Biosciences, OHSU School of Dentistry

Mentor: Luiz Bertassoni

Co-Authors: Alexander E. Davies¹, Rebekka Duhon¹, Joshua M. Moreau^{1,3,4}, Ellen M. Langer^{1,5}, and Luiz E. Bertassoni^{1,2,3,6,7}

1. Cancer Early Detection Advanced Research Center (CEDAR), Knight Cancer Institute, OHSU; 2. Department of Biomedical Engineering, School of Medicine, OHSU; 3. Division of Oncological Sciences, School of Medicine, OHSU; 4. Department of Dermatology, School of Medicine, OHSU; 5. Molecular and Medical Genetics, School of Medicine, OHSU; 6. Division of Biomaterials and Biomechanics, School of Dentistry, OHSU; 7. Center for Regenerative Medicine, OHSU.

Introduction:

The specific communication of multiple cell types in the tumor microenvironment plays a critical role in cancer progression. Current engineering methods have failed to adequately replicate the complexities of the tumor microenvironment (TME). In particular, generating engineered tissue-like environments with multiple TME cell types has remained challenging. Here we demonstrate the capability to pattern complex single cell circuit configurations, using a novel microfluidic bioprinting method, to study cell-cell communication in the early TME.

Methods:

A microfluidic dispenser (Biopixlar, Flucell AB) was optimized to determine the delivery pressure (5 – 80 mbar), internal vacuum (0 – 80 -mbar), and external vacuum (0 – 80 -mbar) to enable highly controllable deposition of single cells suspended in complete media supplemented with polyethylene glycol (15 mg/mL, 1:1) at 1×10^6 cells/mL. Flow conditions were optimized for human cells: MDA-MB-231, MCF7, PC3, breast epithelial cells (MCF10a), fibroblasts, cancer associated fibroblasts, THP-1 derived macrophages, CD4+ T cells, CD8+ T cells, human umbilical vein endothelial cells (HUVECs), and mesenchymal stem cells. As proof of concept, the optimized settings were used to replicate a 2D tumor biopsy region of interest with high spatial precision. Next, cell-cell communication circuits were fabricated with cancer cells (PC3 or MDA-MB-231) and HUVECs. Communication circuits were bioprinted as 4 by 4 cell arrays, with 100 μ m spacing between each cell, equal number of HUVECs and cancer cells, and three different cellular arrangements: alternating cell types, like cell types grouped, and groups of four like cell types. The circuits were live cell imaged for up to 30 hours to observe cell migration patterns, proliferation, and morphological changes as a function of cell-cell communication circuit arrangements.

Results:

Optimal printing parameters were identified as 80 mbar delivery pressure, -25 mbar internal vacuum, and -55 mbar external vacuum. These parameters maintained >99% cell viability and ± 10 μ m spatial precision of printed cells. Live cell imaging of circuits containing PC3s or MDA-MB-231s with HUVECs on collagen substrates revealed changes in migration patterns, proliferation, and morphology depending on the

surrounding cellular arrangement. HUVECs were highly migratory throughout the duration of the experiment, frequently extended protrusions towards nearby HUVECs, but did not display the same level of interaction with PC3s as they did with MDA-MB-231s. In MDA-MB-231 circuits, irrespective of patterning, we identified clear tendencies of HUVECs to herd MDA-MB-231s, travel otop of MDA-MB-231s, collect and carry visible particles released from MDA-MB-231s, and maintain dendritic morphology instead of undergoing the expected vascular tubulogenesis. We found that HUVECs had the best morphology when clustered in groups of four and proliferated most when surrounded by MDA-MB-231s (alternating pattern). We found that MDA-MB-231s only proliferated when surrounded by HUVECs and had the least displacement when surrounded by like cells.

Conclusions:

These results demonstrate a method to precisely bioprint single cell circuits, enabling the investigation of cellular spatial organization and composition within the tumor microenvironment as it relates to tumor initiation and progression.

**PORT (Portland Oral Health Research Training) T90/R90 Program is an OHSU School of Dentistry training program, funded by NIH/NIDCR, that supports mentored training in oral and craniofacial health research to PreDoctoral, Dual Degree, PostDoctoral, and Foreign-Trained Dentist trainees.*

Differential pericyte marker expression in craniofacial benign and malignant vascular tumors

Ginny Ching-Yun Hsu

Assistant Professor, Dept of Oral & Craniofacial Sciences, OHSU School of Dentistry

Co-Authors: Jaster Szu-Wei Lin, Amy Z. Lu, B.S. Dave Chandra D.D.S., Ph.D., Srinivasa R. Chandra, M.D., B.D.S., FDS, FIBCSOMS., Aaron W. James M.D., Ph.D., Ginny Ching-Yun Hsu B.D.S., M.S.

Introduction:

Abnormal development of blood vessels can lead to angioma or vascular tumor in head, neck, and craniofacial areas in early childhood. Hemangioma, benign vascular tumors, derived from blood vessel cell associating the endothelium vascular lumen and basement membrane stabilization by pericyte proliferation. Pericyte markers, PDGFR α , CD146, CD105, CD90, and α SMA, have shown associated and been recognized in specific pericytes and ontogenies. To determine vascular tumor or hemangioma development in soft tissue and bone, histomorphometric pericyte markers associating with aggressive malignancies were demonstrated to reveal the role of pericyte in hemangioma progression and differentiation in benign and malignant vessel tumors.

Methods:

Vascular tumor cases were identified by retrospective chart review of the pathology tissue archives at the Oregon Health & Science University Department of Oral Pathology using the search term “hemangioma” and “angiosarcoma”. Patient demographics such as sex, age at presentation, and tumor location were obtained, as shown in Table 1. Formalin-fixed paraffin-embedded (FFPE) tumor tissue was acquired from the tissue archives, under OHSU IRB approval # STUDY00024205.

For immunofluorescent staining, all sections were blocked with 5% goat serum in phosphate-buffered saline (PBS) for one hour at room temperature (RT). The primary antibodies utilized are as follows: anti- α SMA, anti-CD146, and anti-CD31 (Table 2) for overnight incubation at 4 $^{\circ}$ C. Next, anti-rabbit Alexa Fluor 594-conjugated and anti-mouse Alexa Fluor 488-conjugated antibodies were incubated for 1 hr at RT. DAPI mounting medium was used (Vector laboratories, Burlingame, CA) and visualized by Apotome 3 microscope (Zeiss, Thornwood, NY).

All images for quantification were obtained with Apotome 3 microscopy (Carl Zeiss Microscopy GmbH). CD146, α SMA, CD31, and DAPI were quantified by ImageJ software using five random vessels under 40x microscopical fields per sample. 3 to 4 random images within the encompassed, distinct areas in each lesion were elected, and relative staining intensity was quantified using ImageJ software.

Results:

Perivascular stem cell markers, CD146 and α SMA, were examined in soft tissue, intraosseous, malformation, and angiosarcoma specimens. In immunofluorescent staining, pericyte cells were demonstrated in intraosseous hemangiomas, but not angiosarcomas indicating CD146 and α SMA highly expressed in intraosseous specimen.

Comparing the pericyte marker CD146, soft tissue hemangiomas in comparison to angiosarcoma samples showed no significant difference. Compared to intraosseous hemangiomas, soft tissue hemangiomas

demonstrated a 20.35% decrease in CD146 immunoreactivity and angiosarcomas demonstrated a 26.45% decrease in CD146 expression.

Comparing the pericyte marker aSMA immunostaining, soft tissue hemangiomas in comparison to angiosarcoma specimens showed no significant difference. Compared to intraosseous hemangiomas, soft tissue hemangiomas demonstrated a 25.13% decrease in aSMA immunoreactivity and angiosarcomas demonstrated a 25.13% decrease in aSMA immunostaining.

Conclusions:

Pericyte cells are essential for normal tissue development and repair and associated with vascular tumor formation and progression. The differential expression of CD146 and aSMA in pericytes demonstrates in vascular tumors further suggests that perivascular stem cell numbers are associated with tumor malignancy.

The building blocks of eye lens beta-crystallins are hetero-dimers

Kirsten Lampi, M.Sc., Ph.D.

Professor, Biomaterial & Biomedical Sciences, OHSU School of Dentistry

Co-Authors: Amber D Rolland, PhD, University of Oregon; Takumi Takata, PhD, Kyoto University; Micah T Donor, PhD, University of Oregon; Larry L David, PhD, Chemical Physiology and Biochemistry, OHSU; James S Prell, PhD, University of Oregon.

Introduction:

The purpose of this research was to determine the stoichiometry and structures of the beta-crystallin hetero-oligomers associated with the beta-high fraction. Crystallin fractions isolated from human donor lenses predict higher-ordered oligomers of octamers and higher. Yet, these oligomers have not been characterized in vitro.

Methods:

Groundbreaking work using native ion mobility-mass spectrometry (IM-MS) previously showed the utility of this technique for analyzing α -crystallins, and the present study investigates the application of this technique to β -crystallins, including dimerization kinetics experiments and state-of-the-art molecular dynamics simulations for accurate interpretation of IM-MS collision cross section information.

Results:

Our results show that β -crystallins readily form heterodimers that can be detected by native mass spectrometry at even micromolar concentrations, and that dimers are the building blocks for larger oligomers. Ion mobility experiments and molecular dynamics simulations further reveal that all oligomers identified in these experiments are compact (as opposed to quasi-linear or planar), in agreement with previously published hydrogen-deuterium exchange data obtained by the authors.

Conclusions:

While concentrations used are much lower than that found in the native lens, the detection of higher-ordered hetero-oligomers matches the size of oligomers present in the betaHigh-fraction isolated from human donor lenses. These results help to understand how the eye lens may establish a refractive gradient by tuning β -crystallin oligomer composition and lay the groundwork for future studies measuring the oligomeric structure of β -crystallins derived from both normal and cataractous lenses.

Faster biomineralization and osteogenesis on-a-chip using 3D bioprinting and microfluidics

Rahul Madathiparambil Visalakshan

PostDoctoral Fellow, Bertassoni lab,

Dept of Oral Rehabilitation & Integrative Biosciences, OHSU School of Dentistry

Mentor: Luiz Bertassoni

Co-Authors: Rahul M Visalakshan, Mauricio Sousa, Maria Elisa Lima Verde, Anthony Taheri, Avathamsa Athirasala, Luiz Bertassoni

Introduction:

Bone defects can occur after trauma, infection, or oncologic resection and autologous bone grafting is the current treatment option. However, this method has its limitations in more severe injuries as it may cause infection and scarring at donor sites. Thus, developing biomaterials that are osteoinductive with live cells is essential for treating bone defects.

Methods:

We recently found that embedding human mesenchymal stem cells (hMSCs) within nanoscale-mineralized collagen constructs promotes osteogenic differentiation more than conventional supplements do. However, the current biomineralization process takes 3 days to mineralize. To further enhance the regenerative capacity of these materials and reduce the mineralization time, we developed a microfluidic cell culture system and reduce the mineralization time from 3 days to 3 hours. In this study, we developed a microfluidic cell culture system that recapitulates biomineralization and early osteogenesis on injectable microgels. We used a DLP (Digital light processing) printer to 3D bioprint microgels of GelMA encapsulated with hMSCs. These microgels were mineralized under flow within 3 hours with calcium and phosphate rich media, in a custom-made chip.

Results:

We characterized the mineralization of microgels by alizarin red and von Kossa staining. Live/dead staining showed hMSCs viability after mineralization underflow, while OCN, RUNX2 & PDPN expression indicated successful osteogenic stem cell differentiation in the presence of fluid shear stress (FSS).

Conclusions:

Our novel approach provides an effective strategy for developing treatments for bone defects by recapitulating biomineralization and osteogenesis on an injectable microgel.

Butyrolactone-Ladderane Biosynthetic Gene Cluster Influences Streptococcus mutans Cariogenic Factors

Stephanie Momeni

PostDoctoral Fellow, Wu lab, Dept of Oral Rehabilitation & Integrative Biosciences, OHSU School of Dentistry

Mentor: Hui Wu

Co-Authors: S. S. Momeni, M. Loop, B. Xie, H. Wu

S.S. Momeni, B. Xie, H. Wu, Oral Rehabilitation & Integrative Biosciences,
Oregon Health and Science University, Portland, Oregon, UNITED STATES;

M. Loop, Pharmacology & Toxicology, University of California Berkeley, Berkeley, California, UNITED STATES.

Introduction:

The butyrolactone gene of the butyrolactone-ladderane biosynthetic gene cluster (BL-BGC) identified in *Streptococcus mutans* clinical strain UAB-10 has been shown to impact biofilm pH, a key cariogenic factor. The BL-BGC was identified in the prevalent clinical *S. mutans*-genotype G18 from a high-caries risk population of African American children. The purpose of this study was to determine the impact of the BL-BGC in *S. mutans* on cariogenic potential and fitness.

Methods:

Biofilms were used to assess biofilm biomass using crystal violet assay (16 hours, Todd Hewitt+1% sucrose). Oxidative stress response was evaluated using spot competition assay with hydrogen peroxide discs and 20 ml fresh sub-cultured bacteria. To determine in-vivo colonization, a *Drosophila melanogaster* model was utilized with 2-day antibiotic, followed by 3-days (twice daily) capillary feeding of *S. mutans* in 5% sucrose. Preliminary metabolomics analysis was performed to assess metabolic differences between parent and mutant strains.

Results:

S. mutans BL-BGC mutant demonstrated a significant reduction in biofilm biomass compared to parent strain. The BL-BGC parent strain was significantly more resistant to oxidative stress than mutant by competition assay. Preliminary data for the fly colonization model indicates the parent strain, UAB-10, colonizes flies better than BL-BGC mutant. Preliminary metabolomics data indicates a significant impact on metabolite feature profiles for mutants compared to the parent strain.

Conclusions:

Presence of BL-BGC increases *S. mutans* ability to survive oxidative stress, offering protection from hydrogen peroxide producing commensal oral microbiota. Loss of BL-BGC dramatically reduces biofilm biomass, reduces ability of *S. mutans* to colonize in the fly model, and globally impacts the metabolic profiles for single species, static biofilms. Collectively, these findings suggest presence of the BL-BGC has significant impact on *S. mutans* virulence traits and fitness. Further study is needed with polymicrobial models and to determine if BL-BGC can be used as biomarker for caries risk assessment.

Plasmalogen, a glycerophospholipid crucial for *S. mutans* acid tolerance and colonization

Rong Mu

Senior Research Associate, Wu lab, Dept of Oral Rehabilitation & Integrative Biosciences,
OHSU School of Dentistry

Co-Authors: Stephanie Momeni, Xixi Cao, Baotong Xie and Hui Wu

Introduction:

Plasmalogen is a specific glycerophospholipids found in both animals and bacteria. It plays a critical role in eukaryotic cellular processes and is closely related to certain human diseases, including neurological disorders and cancers. However, little is known about its biological role in bacteria. To investigate whether plasmalogen plays important roles in oral microbiota, we identified a plasmalogen producing gene in a cariogenic *Streptococcus mutans* and examined its role in stress tolerance and bacterial colonization in vivo in a fly model.

Methods:

A markerless deletion strain of SMU_438c was generated through chromosomal mutagenesis, and plasmalogen production was detected by using Schiff's reagent in both colonies and planktonic cells. Heterogeneously expressing SMU_438c in a plasmalogen negative bacterium was done by transforming a shuttle vector expressing SMU_438c into the strain. Acid tolerance was examined by acid killing assay and biofilm staining. Bacterial colonization in vivo was examined by using a fly model.

Results:

We identified SMU_438c as the plasmalogen producing enzyme in *Streptococcus mutans* under anaerobic condition. Expressing SMU_438c in a plasmalogen negative strain, *Streptococcus sanguinis*, led to the production of plasmalogen. The plasmalogen deficient strain exhibited significant lower acid tolerance and significant decrease in bacterial colonization of flies compared to the wild-type strain.

Conclusions:

SMU_438c is responsible for the production of plasmalogen in *Streptococcus mutans* under anaerobic condition and the bacterial plasmalogen seems to play important roles in bacterial stress tolerance and in vivo colonization.

Integrating Dental Gross Anatomy and Flipping it on its Head

Sylvia Nelsen

Assistant Professor, Dept of Oral Rehabilitation & Integrative Biosciences, OHSU School of Dentistry

Introduction:

Previously, students learned human anatomy in two phases – an introductory “Gross Anatomy” course focusing on regions below the neck followed by an intensive “Head & Neck Anatomy” course. This regional approach is traditional; it’s the easiest way to align content with progression through dissection. However, it cognitively separates the head and neck from the rest of the body, which is not how biology functions. The nervous system influences every system, functional systems are rarely confined to one region, and an important oral-systemic connection has repeatedly been demonstrated in health and disease (Byrd et al., 2021 and references therein). For this reason, an integrated gross anatomy course was developed, and a flipped classroom format for learning was chosen.

Methods:

In order to increase students’ internal motivation to participate in a non-traditional course, it is important to communicate not only the what and how, but also the why (Blessner et al., 2014). With this aim in mind, an orientation to what the course topics are, how they are organized, and why they are organized that way – to improve understanding of the oral-systemic connection – was presented to the students. Similarly, an explanation of what the course resources are, how students should use them in a flipped classroom environment, and why this learning environment is being used for the course – to allow students to learn at their own pace and increase the efficiency and effectiveness of in-class time – was provided during orientation. At the end of the course, anonymous student comments regarding strengths of the course and areas for improvement were analyzed using qualitative analysis software (ATLAS.ti) to look for themes related to these two topics with the aim of determining whether an integrated anatomy course taught using a flipped classroom format is feasible and acceptable in the OHSU DMD program. Following up on the course evaluation data, an anonymous survey was sent to further inquire about time spent, resources used, perceptions of preparedness, and any suggestions for improving the effectiveness of the emphasis on the oral-systemic connection and the learning experience overall.

Results:

Survey results were analyzed, and qualitative analysis of anonymous student comments in response to two prompts was performed. In response to the prompt, “What are the strengths of the course?” one theme that emerged was student appreciation for the quality and variety of resources provided. Survey results indicated that, although all resources were used to some degree, students primarily studied from faculty-generated content and almost never used the assigned textbook or atlas. In response to the prompt, “What recommendations do you suggest for improving the course?” one theme that emerged was insufficient time to complete the pre-work. Survey responses indicated that nearly half of students spent 3-5h doing pre-work, which is expected given the credit hours for this course, suggesting that communication to better align student expectations may be warranted. Though comments in the course evaluation failed to acknowledge the emphasis on oral-systemic connection, 80.6% of respondents indicated that they “strongly” or “somewhat agree” that the course topics and the order in which they were presented helped them understand the connection.

Conclusions:

Student comments suggested that, with some modifications, the course could be both feasible and acceptable. Survey results helped clarify student comments and provide a basis for data-informed course revisions. The same process of data analysis will be completed with a second cohort to determine (a) whether students recognized the functional connections between oral and systemic anatomy, (b) whether students perceived the active learning strategies as beneficial, and (c) how the course can improve in both aspects. The goal is to increase the feasibility and acceptability of an integrated anatomy course taught using a flipped classroom format, and to ultimately improve student performance.

Investigating the Effects of Microfluidic Technology on the Biomineralization of Collagen Scaffolds in Bone-on-a-Chip.

Jonathan Nguyen

DMD Student, OHSU School of Dentistry

Mentor: Luiz Bertassoni

Co-Authors: Jonathan Nguyen*, B.S 1; Rahul Madathiparambil Visalakshan, MBiotech, Ph.D 1; Mauricio Gonçalves da Costa Sousa, DDS, MS, Ph.D 1; and Luiz E. Bertassoni, DDS, Ph.D 2,1.

1. Div of Biomaterials & Biomechanics, Dept of Restorative Dentistry, OHSU School of Dentistry, 2 Cancer Early Detection Advanced Research (CEDAR), Knight Cancer Institute Portland, OR, USA

Introduction:

Bone is a dense, vascularized connective tissue, composed in a matrix of living cells and non-living matter. Currently, strategies to mimic native bone tissue in-vitro have drawn attention to the bioengineering community due to the drawbacks associated with bone autografting, including increased risk of infection, limited donor-site supply, and morbidity. We believe the process and time of forming hydroxyapatite at the inter-and-intra fibrillar collagen network can be reduced by incorporating microfluidics to enable key features found in a bone microenvironment compared to conventional in-vitro or suspended bone models which fail to replicate the complexity of native bone.

Methods:

This study looks to create a biomaterial capable of achieving the definitive characteristics of bone tissue and extracellular microenvironment by fabricating and optimizing its biomineralization property. Previous work done by our group (Thrivikraman et al, Nature Communications 2019) achieved nanoscale biomineralization of collagen scaffolds within 72 hours under static conditions. Here we used a microfluidic approach to improve the nanoscale mineralization efficiency of collagen hydrogels by using a custom-built chip with a flow rate of 15 mL/hr. Collagen mineralization was characterized by bright field imaging and Alizarin Red S staining. Furthermore, TEM image analysis was employed to observe the inter-and-intra fibrillar nanoscale mineralization.

Results:

We successfully developed a CAD design and laser cut the molds to cast PDMS chips with precision, while assembling the acrylic base with different sealing conditions to optimize the flow parameters and prevent leaking in the microfluidic system. Bright field microscopy images displayed the dark complexion on the collagen after flowing mineralization media for 12 hours with a 15 mL/hr flow rate confirming the mineralization. Further TEM image analysis verified the mineralization penetration and deposition of hydroxyapatite and the formation of inter-and-intra fibrillar crystallites.

Conclusions:

Ultimately, this efficient approach allows for rapid synthesis of bone-like tissue models that may enable future developments within the field of bone engineering. Henceforth, the future direction of this study is threefold: 1) to utilize Fourier Transform Infrared spectroscopy to characterize the chemical composition of our mineralized sample with that of native bone tissue 2) encapsulate human mesenchymal stem cells into the collagen scaffolds and determine if matrix stiffness remains to stimulate osteogenic differentiation 3) compare and contrast different types of flow rates to optimize the mineralization of these collagen scaffolds.

Laser based-bioprinting of large 3D heterogenous tissues with vascular networks using poly(N-isopropylacrylamide) as sacrificial templates

Narendra Singh

Senior Research Associate, Bertassoni lab,
Dept of Oral Rehabilitation & Integrative Biosciences, OHSU School of Dentistry

Mentor: Luiz Bertassoni

Co-Authors: Anthony Tahayeri^{1,2}, Abhinay Mishra^{1,2}, Haylie Helms^{2,4}, Luiz E. Bertassoni^{1,2,3,4}

¹Department of Restorative Dentistry, School of Dentistry, Oregon Health & Science University, Portland, OR

² Cancer Early Detection Advanced Research Center (CEDAR), Knight Cancer Institute, Portland, OR

³Center for Regenerative Medicine, School of Medicine, Oregon Health & Science University, Portland, OR

⁴ Dept of Biomedical Engineering, School of Medicine, Oregon Health & Science University, Portland, OR

Introduction:

Sacrificial templates for fabricating perfusable vascular networks in engineered tissues have been constrained in architectural intricacy due to the limitations of current extrusion-based 3D printing techniques. Most liquid-phase materials deposited by extrusion are subject to deformation or collapse under their own weight, and their viscosity and surface tension make precise dispensing of small volumes challenging. Here, we show the synthesis and printing of on demand dissolvable photo-PNIPAM that can be patterned with algorithmically generated vessel-like networks and other complex hierarchical structures using laser-based bioprinting.

Methods:

In brief, the prepolymer solution to fabricate thermoreversible poly(N-isopropylacrylamide) (photo-PNIPAM) degradable dendritic networks and complex sacrificial structures were prepared dissolving NIPAM in dimethyl sulfoxide or isopropanol containing phosphate buffer saline and photoinitiator. Furthermore, the various type of sacrificial complex structures was fabricated using digital light-based printer and the optimized prepolymer.

Results:

The composition of prepolymer precursor, solvent ratio and light exposure time were optimized to modulate dissolution and stability of printed complex photo-PNIPAM structures in PBS at 4°C and 37 °C, respectively. Moreover, cell viability and proliferation were evaluated on to the surface of the photo-PNIPAM and results confirm the higher cell viability of HUVECs and MSCs.

Conclusions:

This light-based strategies of degradable photo-PNIPAM printing may help to enable fabrication of sustain thick and dense cellularized engineered tissues with complex and heterogenous perfusable vasculature networks.

Development of a bone-like microenvironment on-a-chip to simulate osteoclastogenesis

Mauricio Sousa

PostDoctoral Fellow and PORT R90 Trainee*, Bertassoni lab,
Cancer Early Detection Advanced Research (CEDAR), Knight Cancer Institute;
OHSU School of Dentistry Dept of Oral Rehabilitation & Integrative Biosciences, OHSU School of Dentistry

Mentor: Luiz Bertassoni

Co-Authors: Maria Elisa Lima Verde^{1,4}, Avathamsa Athirasala^{1,4}, Rahul Visalakshan^{1,4}, Cristiane Franca Miranda^{1,4}, Luiz Eduardo Bertassoni¹⁻⁴.

1 Cancer Early Detection Advanced Research (CEDAR), Knight Cancer Institute.

2 Center for Regenerative Medicine, OHSU School of Medicine.

3 Department of Biomedical Engineering, OHSU School of Medicine.

4 Division of Biomaterials and Biomechanics, Department of Restorative Dentistry, OHSU School of Dentistry

Introduction:

Osteoclasts are multinucleated cells of myeloid origin responsible for bone remodeling during physiological and pathological craniofacial events such as bone growth, healing, infection, and metastasis. These cells coordinate with other bone cells, particularly osteoblasts and osteocytes. However, despite the large body of work, most of the current in vitro models for osteoclastogenesis fail to mimic the bone complexity, which has osteocytes and osteoblasts in a 3D intrafibrillarly mineralized matrix. Furthermore, the existing protocols to differentiate osteoclasts require the use of expensive external osteoclastogenic proteins, for example, receptor activator of nuclear factor kappa-B ligand (RANK-L) and macrophage colony-stimulating factor (MCS-F), to obtain osteoclasts in 14 days.

Methods:

We hypothesize that engineering a biomimetic bone environment with the proper cues from the extracellular matrix and bone cells is enough to accomplish faster osteoclast differentiation without external stimulants. To that end, we engineered a biomimetic bone environment on-a-chip in which human osteoblast-laden matrices (3x10⁶ cells/mL) with collagen (2.5 mg/mL⁻¹) were mineralized for three days in a solution of CaCl₂·2H₂O, osteopontin, and K₂HPO₄. We then co-cultured macrophages (2x10⁵ cells/mL⁻¹) and human osteoblasts (2x10⁴ cells/mL⁻¹) in contact with the 3D mineralized matrix as it happens in the native bone.

Results:

After seven days, we observed the presence of multinucleated cells positive for tartrate-resistant acid phosphatase (TRAP), confirming the effectiveness of the osteoclastogenesis process on the bone on-a-chip without any external supplement. Also, MMP9 was highly expressed in both treated and non-treated groups with RANK-L and MCS-F by immunofluorescence. Furthermore, pit areas in the mineralized matrix were observed, suggesting a functional osteoclastogenic activity.

Conclusions:

In conclusion, we anticipate that this system can be a promising tool to understand bone biology and craniofacial disorders in vitro.

**PORT (Portland Oral Health Research Training) T90/R90 Program is an OHSU School of Dentistry training program, funded by NIH/NIDCR, that supports mentored training in oral and craniofacial health research to PreDoctoral, Dual Degree, PostDoctoral, and Foreign-Trained Dentist trainees.*

The role of the gene polychaetoid in aging

Baotong Xie

Research Assistant Professor, Dept of Oral Rehabilitation & Integrative Biosciences, OHSU School of Dentistry

Mentor: Hui Wu

Co-Authors: Rong Mu, Stephanie Momeni, Hui Wu

Introduction:

Aging is a multi-factorial process regulated by a combination of genetic and environmental factors. There is accumulating evidence that gut microbiota plays a significant role in longevity across species. Notably, host genetics is an important determinant of the gut microbiota composition and abundance. Mechanistic elucidation of the cause and effect relationships between host genetics, gut microbiota dynamics and host health outcomes have enormous biomedical significance. However, due to the complexity of the mammalian gut microbiota, understanding how the host age-related genetics affects the gut microbiota to influence the host aging at the organismal level has remained a challenging question.

Methods:

A wealth of available genetic and molecular resources, the simple taxonomic composition of the gut microbiota and a relatively short life span have made *Drosophila* a powerful model organism in the gut microbiota, genetic and aging studies. We took advantage of the powerful genetic tools in *Drosophila* to identify the genetic factors that influence aging. We also used behavior assay, intestinal barrier assay, RT-PCR and other molecular tools to analyze the aging-related physiology in *Drosophila*. In addition, in vitro bacteria culture, 16s RNA gene sequencing methods are used to analyze the commensal bacteria in *Drosophila* gut.

Results:

We have identified a *Drosophila* adhesion protein-coding gene *polychaetoid* (*pyd*) significantly affects life span. We found that the abundance and composition of commensal bacteria in the *pyd* mutant flies were increased. In addition, weaker locomotor activities that the control flies were observed in the *pyd* mutant flies. We further found that removal of commensal bacteria in *pyd* mutant flies significantly extend the life span, indicating commensal bacteria changes in *pyd* mutant contribute to the life span reduction.

Conclusions:

The cell junction coding gene *pyd* plays an important role in aging in *Drosophila*. Loss of *pyd* leads to increase in the abundance and composition of the commensal bacteria, and these gut microbiota changes contributes to the loss of *pyd*-related lifespan reduction.

Structural and functional insight into biofilm regulatory protein in *Streptococcus mutans*

Hua Zhang

Instructor, Dept of Oral Rehabilitation & Integrative Biosciences, OHSU School of Dentistry

Co-Author: Hui Wu

Introduction:

Streptococcus mutans is a major contributor to the development of dental caries. Biofilm regulatory protein A (BrpA) is important for *S. mutans* cariogenic virulence. But how it works on the biofilm is still unknown.

Methods:

Recombinant BrpA and fluorescent tagged BrpA proteins were constructed, expressed in *E. coli* and purified by His Trap column and size-exclusion chromatography. *S. mutans* biofilms formed in the presence of the fluorescently tagged BrpA were stained by Dextran conjugated CasBlue, Propidium iodide and Nile Red. The purified BrpA protein was crystallized by a hanging drop method, and its structure was solved by molecule replacement. Binding kinetics were measured by microscale thermophoresis (MST) using Monolith (NanoTemper).

Results:

In this study, we demonstrated the purified BrpA rescued the biofilm defect from the BrpA knockout strain. Co-localization study of the biofilms revealed that BrpA is associated with glucan. The binding assay indicated the BrpA protein directly interacts with the glucan producing Gtf enzymes. We solved the X-ray structure of BrpA at 1.8 Å. The structure uncovered a lipid binding motif conserved among BrpA homologs. In addition, we found that positive charged amino acids on the BrpA surface are critical for binding Gtfs and important for the biofilm formation.

Conclusions:

BrpA regulates the biofilm formation of *S. mutans* through its interaction with Gtfs. The positive charged amino acids on the surface of BrpA protein are important for the interaction. Our study revealed a previously unknown mechanism underlying the BrpA function in mediating *S. mutans* biofilms.